Article (refereed) - postprint

Durand, Alexis; Maillard, François; Foulon, Julie; Gweon, Hyun S.; Valot, Benoit; Chalot, Michel. 2017. **Environmental metabarcoding reveals contrasting belowground and aboveground fungal communities from poplar at a Hg phytomanagement site.** *Microbial Ecology*, 74 (4). 795-809. https://doi.org/10.1007/s00248-017-0984-0

Environmental metabarcoding reveals contrasting belowground and aboveground fungal communities from poplar at a Hg phytomanagement site

Alexis Durand[a], François Maillard[a], Julie Foulon[a], Hyun S. Gweon[b], Benoit Valot[a], Michel Chalot[a, c*]

[a] Laboratoire Chrono-Environnement, UMR 6249, Université de Bourgogne Franche-Comté, Pôle Universitaire du Pays de Montbéliard, 4 place Tharradin, BP 71427, 25211 Montbéliard, France

[b] Centre for Ecology & Hydrology, Maclean Building, Benson Lane, Crowmarsh Gifford, Wallingford, Oxon OX10 8BB, UK

[c] Université de Lorraine, Faculté des Sciences et Technologies, BP 70239, 54506 Vandoeuvre-les-Nancy, France

*Corresponding author: Laboratoire Chrono-Environnement, UMR 6249, Université de Bourgogne Franche-Comté, Pôle Universitaire du Pays de Montbéliard, 4 place Tharradin, BP 71427, 25211 Montbéliard, France

Tel: +33 3 81 99 46 76, Email: michel.chalot@univ-fcomte.fr

Abstract

Characterization of microbial communities in stressful conditions at a field level is rather scarce, especially when considering fungal communities from aboveground habitats. We aimed at characterizing fungal communities from different poplar habitats at a Hg-contaminated phytomanagement site by using Illumina-based sequencing, network analysis approach and direct isolation of Hg resistant fungal strains. The highest diversity estimated by the Shannon index was found for soil communities, which was negatively affected by soil Hg concentration. Among the significant correlations between soil OTUs in the co-occurrence network, 80 % were negatively correlated revealing dominance of a pattern of mutual exclusion. The fungal communities associated with *Populus* roots mostly consisted of OTUs from the symbiotic guild, such as members of the *Thelephoraceae*, thus explaining the lowest diversity found for root communities. Additionally, root communities showed the highest network connectivity index, while rarely detected OTUs from the *Glomeromycetes* may have a central role in the root network. Unexpectedly high richness and diversity were found for aboveground habitats, compared to the root habitat. The aboveground habitats were dominated by yeasts from the *Lalaria*, *Davidiella* and *Bensingtonia* genera, not detected in belowground habitats. Leaf and stem habitats were characterized by few dominant OTUs such as those from the *Dothideomycete* class producing mutual exclusion with other OTUs. *Aureobasidium pullulans,* one of the dominating OTUs, was further isolated from the leaf habitat, in addition to *Nakazawaea populi* species, which were found to be Hg resistant. Altogether, these findings will provide an improved point of reference for microbial research on inoculation-based programs of tailings dumps.

Keywords : Hg-enriched tailings dump, Hg resistance, internal transcribed spacer metabarcoding, poplar microbiome, Illumina MiSeq, network.

Introduction

Plants in natural and agricultural settings are colonized by a wide range of microbes on both their outer and inner surfaces [1]. Nevertheless, the scientific understanding of the microbial communities of woody species is quite limited, especially for microbes associated with aboveground tissues. Many tree tissues may indeed represent distinct microbial habitats, such as the rhizosphere, the root and leaf endospheres, the episphere of the phyllosphere and fruits, flowers, leaves, buds, stems, branches or even the trunk [2, 3]. Moreover, some of the microorganisms that colonize these habitats establish strong links with their host, whose disruption may result in loss of host fitness [4]. For instance, a certain groups of mycorrhizal fungi that form symbiotic association with the root system, are of a importance for tree nutrition and health, as they play key roles in the carbon and nitrogen cycles [5]. In the phyllospheric habitat, archaea, bacteria, filamentous fungi and yeasts have been identified , although less work has been done on the two latter groups of microorganisms [6]. Studies are increasingly indicating that fungi influence the fitness of their host plants, either negatively by acting as pathogens [7], or positively by increasing the stress tolerance of the plant [8], shaping insect herbivory [9] or reducing the infection of plant tissues by pathogens [10].

Trees, as perennials, are made of a variety of habitats that may host contrasted microbial communities, which composition and diversity may vary with season, age, species, climatic conditions. Therefore, they are relevant models for studying the structure and composition of microbial communities, but until recently, our knowledge has been limited due to the difficulty of adequately describing microbial communities with classical culture-dependent methods. The recent development of massively parallel 454 pyrosequencing [11, 12] and ion torrent sequencing [13], combined with DNA multiplexing, provides an opportunity to explore parts of the microbiome that are otherwise unreachable through culture-dependent approaches [14]. Microbiomes associated with belowground and aboveground tree habitats have been screened

69 at a large spatial scale using these technologies in some cases, and several studies revealed the
70 potential of the host tree genotype and environmental conditions to induce the establishment of
71 specific microbial communities [11, 15–17]. More recently, new high-throughput technologies,
72 such as the Illumina sequencing platform, have become available, showing a far greater
73 sequencing capacity, producing millions of sequences, which leads to much greater depth of
74 coverage of microbial [18]. It is now possible to examine the full extent of the richness and
75 diversity exhibited by microorganisms in different habitats. However, the quantity of data
76 reaches a critical point at which previous approaches are insufficient to decipher the structure
77 of complex microbial communities. Network analysis of significant taxon co-occurrence
78 patterns may help to decipher the structure of complex microbial communities among various
79 habitats. Software such as CoNet has been developed and optimized specifically to detect
80 significant non-random patterns of co-occurrence (co-presence and mutual exclusion) using a
81 Reboot method to determine the significance of each associations in the network [19]. Network
82 analysis requires lot of samples replication to obtained strong statistical analysis leading to
83 trustable correlations. This computation method combined with adapted experimental design
84 and with the tremendous amount of metadata obtained by high throughput sequencing
85 technologies gives us the opportunity to explore communities with a new global tool to revealed
86 OTUs importance in the community.

87 Within the growing environmental pollution paradigm, poplar is a keystone tree used as
88 feedstock for biofuel production and as a biological tool for phytoremediation and revegetation
89 [20]. The term phytoremediation refers to the use of plants and associated microorganisms to
90 eliminate, attenuate or restrain environmental damage or threats posed by a contaminant. Hg is
91 a contaminant classified within the quantitatively most important pollutant groups known as
92 trace elements (TEs). It is highly persistent in the soil environment and is classified as a
93 “priority hazardous substance” by the Agency for Toxic Substances and Disease Registry

(ATSDR) due to its toxicity, mobility, and long residence time in the atmosphere *(Available online http://www.atsdr.cdc.gov/SPL/index.html)*. In a previous paper, we focused on characterizing the microbial communities that had naturally recolonized the sediment of a chlor-alkali tailings dump after sediment deposition had ceased. We further demonstrated that most of the Hg detected in the aboveground parts of *Salicaceae* trees collected at that site had entered the poplar leaves through exclusively through an atmospheric pathway [21]. However, the role of aboveground and belowground microbial populations in Hg-contaminated environments remains unknown, and there is a need for a holistic ecosystem-level understanding of microbial communities associated with poplar [22].

In this study, we collected soil and tree samples from the belowground and aboveground habitats of poplars grown as a short-rotation coppice (SRC) plantation at a Hg-contaminated site, and performed isolation of fungal strains. We combined fungal community analyses using Illumina-based sequencing with network analysis to investigate the composition and assembly of fungal communities in these samples. We expected that we would observe clear differences in the relative abundance and composition of fungal groups across poplar habitats that may improve our understanding of the microbial ecology of these environments. Providing key information on the fungal communities of belowground and aboveground will hopefully be of use for practitioners of bioremediation approaches who often lack of important information such as the effect of the pollutants (in this case heavy Hg) on the microbial communities that surround the flora and fauna. This knowledge may benefit efforts to mitigate the environmental impact of tailing management facilities.

Materials and Methods

Site description and sampling design

The location and history of the site have been fully described elsewhere [13, 23] briefly, the site investigated in the current study was exploited as a sediment storage area from the 1950s to 2003. The sediments originated from effluents produced during electrolytic processes associated with a Hg cell chlor-alkali process. A poplar monoclonal plantation of the cultivar Skado (*P. trichocarpa* x *P. maximowiczii*) was implemented in 2011 as a short-rotation coppice (SRC, 2200 stems/ha). The experimental design thus guaranteed minimum host variation to focus on interactions between microorganisms in various tree habitats. Sampling was carried out in summer 2014, consisting of collecting soil, root, stem and leaf samples from six random trees, selected in three replicated plots (2 trees per plot). Soil samples composed of bulk soils from under the canopy of the trees were sieved to <4 mm. After the removal of litter, the roots were collected from the upper 20 cm layer of soil from under the canopy of the trees. They were separated from the soil via 2 ultra-pure water baths, and the smallest roots were selected and separated from larger roots by cutting them with a scalpel. Branch samples were collected from poplar branches of axe 2 (0.8 to 1.2 cm diameter) at an ca. 5 m height, corresponding to the half-crown of the poplar. Leaf samples were composed of 3 leaves collected from the above branches. All samples were obtained over a one-day period to reduce any heterogeneity imparted by climatic conditions. The samples were either freeze-dried and stored at -20°C for molecular analysis or dried at ambient temperature (24°C ± 1) for physico-chemical analyses. Thus, we considered the belowground and aboveground habitats to include both endophytic and epiphytic fungi.

Molecular methods

Within 2 weeks after sampling, the stored samples were freeze-dried (RP2V, Group S.G.D. France) and ground into a homogenous powder in a Mixer Mill for 3 min at 30 Hz (model MM400; Retsch Inc., Newtown, Pennsylvania, USA). Environmental DNAs were then extracted using a modified hexadecyltrimethylammonium bromide (CTAB)

chloroform/isoamyl alcohol protocol [24, 25] for root, stem and leaf samples, while environmental DNA from the soil samples was extracted with the PowerSoil DNA isolation Kit following the manufacturer's instructions (MoBio Laboratories, Inc., Carlsbad, CA USA). A purification step was added to all samples using the Power Clean® Pro DNA Clean-Up kit (MoBio Laboratories, Inc., Carlsbad, CA USA) to improve the quality of the isolated DNA. DNA quality and quantity were assessed via agarose gel electrophoresis and with the Quant-iT™ PicoGreen® dsDNA Assay Kit (Invitrogen, Carlsbad, CA, USA) using an FLX-Xenius spectrofluorometer (SAFAS, Monaco). Equimolar DNA pools were produced and adjusted to 10 ng/µl. Sequencing of the fungal ITS1 region [17, 26] was performed with the Illumina MiSeq platform (Microsynth AG, Switzerland). PCR amplification of the partial ITS gene was performed using the fungi-specific primers ITS1F (CTTGGTCATTTAGAGGAAGTAA) and ITS2 (GCTGCGTTCTTCATCGATGC) [27]. These primers target a short portion of the fungal ITS region, resulting in an amplicon of small size (~ 300 bp) appropriate for Illumina sequencing.

Bioinformatics and statistical analysis of diversity

Sequence de-multiplexing and bioinformatics processing of the datasets were performed using the PIPITS pipeline [28]. PIPITS is an automated bioinformatics pipeline dedicated for fungal ITS sequences which incorporates ITSx to extract subregions of ITS and exploits the latest RDP Classifier to classify sequences against the curated UNITE fungal data set. Briefly, all raw read pairs were joined at the overlapping region and then quality filtered, chimera filtered, singleton filtered, contaminant filtered, merged and clustered into operational taxonomic units (OTUs), defined at 97% sequence similarity. We excluded singleton OTUs to avoid technical artifacts and overestimation of the number of species [29, 30]. The taxonomic assignment of OTUs was performed using the UNITE [31] database at a 97% similarity

168 threshold. The samples were rarefied to 26 671 sequences. The Shapiro test and the Bartlett test
169 were employed to check the normality and homoscedasticity of the data, respectively. Our data
170 were systematically verified for non-normality and homoscedasticity, and the effects of the
171 compartment on the alpha diversity estimates for the fungal assemblage were examined using
172 the Kruskal-Wallis test. A number of alpha diversity indices (OTU richness, Chao estimation,
173 Shannon diversity index, inverse of the Simpson diversity index, measure of evenness based on
174 the Shannon index and coverage) were calculated using MOTHUR [32].
175 The coverage calculator returns Good's coverage for an OTU definition. Coverage was
176 calculated as: C=[1-(*n*/*N*)]*100 (%), where *n* is the number of OTUs, and *N* is the number of
177 sequences.

178 A 2-dimensional non-metric multi-dimensional scaling (NMDS) was calculated using
179 the Bray–Curtis method (k=3) on the basis of standardized (Wisconsin double) and square root
180 transformation of OTU abundance using the "metaMDS" function in the Vegan package in R.
181 We PERformed a single Multivariate ANalysis Of the VAriance (PERMANOVA), run with
182 1,000 permutations, using the "anosim" function in the Vegan package in R and employed
183 ANalysis Of SIMilarities (ANOSIM) to obtain P-values (i.e., significance levels) and the R
184 value (i.e., the strength of the factors on the samples). These results were paired with a heatmap
185 of Spearman's correlations between the relative abundances created with "heatmap.2" from the
186 gplots package. The numbers of OTUs that were shared between habitats were visualized using
187 Venn diagrams implemented in Mothur with the function "venn". We considered an OTU to be
188 present in a compartment if that OTU was present in at least 25% of the samples from the
189 habitats. Correlations between the diversity parameters and the measured Hg parameters were
190 calculated based on Spearman's product moment correlation coefficient (R^2). Riverplots were
191 created with the "riverplot" function in the riverplot R package. Rarefaction curves were
192 generated with the "rarecurve" function of the Vegan package in R. The bioinformatic analysis

193 was conducted using a computer with the following specifications: Ubuntu, Intel®Core™i7-
194 4790 CPU @ 3.60GHz x8, 16GB RAM.
195
196 ***Network analysis***
197 To construct a network and simplify visualization and interpretation, a separate OTU abundance
198 table was derived using the aforementioned pipeline, but with a different OTU clustering
199 threshold (90%) [33]. Following Weiss and collaborators [34] extremely rare OTUs were
200 filtered out; i.e., for each habitat, all OTUs appearing in less than 25% of samples were
201 discarded, and all OTUs showing a relative abundance of < 0.01% of the total sequences were
202 also discarded. Network construction was performed with the plugin CoNet (v. 1.1.b) [35] in
203 Cytoscape software (v. 3.3.0) [36] following the protocol described by Faust and collaborators
204 [37]. Briefly, for each of the four similarity measures (Bray–Curtis and Kullback–Leibler
205 dissimilarity, Pearson and Spearman correlation), the distribution of all pair-wise scores was
206 computed. Given these distributions, initial thresholds were selected such that each measure
207 contributed 1,000 positive and 1,000 negative edges to the initial network. For each measure
208 and each edge, 1,000 renormalized permutation and bootstrap scores were computed, followed
209 by the measure-specific P-value. Any edges exhibiting scores outside the 95% confidence
210 interval defined by the bootstrap distribution or that were not supported by all measures were
211 discarded as well [34]. The networks were explored and visualized with Cytoscape. Based on
212 the results of Berry and Widder (2014)[38], we have chosen to use the degree as a keystone
213 proxy.

214 ***Hg analysis in the substrate and biomass***

215 Hg was measured in the soil and poplar samples with an AMA-254 cold vapor atomic
216 absorption (CV-AAS) Hg analyzer (Altec Co., Czech Republic), using the standard conditions

recommended by the manufacturer (120 s drying, 150 s heating, 45 s cooling). The validity of the analytical method was checked using the certified reference material (CRM) Oriental Basma Tobacco Leaves (INCT-OBTL-5), with a certified Hg content of 20.9 ± 1.3 ng/g DM [39], and quality controls were regularly performed as described elsewhere [23].

Hg resistant yeast isolation and Hg resistance

Leaves were collected from the field experimental site described above during summer 2015 and 2016, and immediately brought to the laboratory. The yeast were isolated using an enrichment technique on a malt extract medium adapted from a previously described method [40]. Briefly, intact leaves were incubated for 48 hr at 25°C and 200 rpm in an enrichment medium (at pH 3.7 adjusted with lactic acid) containing 30 g/l malt, 5 g/l peptone, 5 ml/l filtered leaf extract, and increasing amounts of $HgCl_2$ at final concentrations of 0, 2, 5, 10 or 20 µM. Hundred µl of leaf samples were then plated on malt extract agar (12 g/l malt) and PDA (Potato Dextrose Agar, sigma) media, supplemented with the corresponding $HgCl_2$ concentrations. The number of growing yeast was expressed in colony forming units (CFU) per ml. The strains growing at 10 µM Hg were purified, and resuspended in liquid malt extract or PDA media supplemented with 35% v/v glycerol and maintained at -80°C for further analysis.

Isolated strains were grown in 8 ml of growth medium for 48h at 27°C on a shaker table (200 rpm). After centrifugation, DNA was extracted from the pellet with the EZNA Bacterial DNA kit (OMEGA bio-tek, USA) in accordance with the manufacturer's instructions. The D1/D2 domain of LSU rRNA was amplified using a PCR with the universal primers ITS-1 (59-TCCGTAGGTGAACCTGCG-39) and NL-4 (59-GGTCCGTGTTTCAAGACGG- 39) [41]. All the ITS PCR products were sequenced by pyrosequencing 454 (Genewiz Beckman Coulter Cenomics, United Kingdom). DNA sequences were edited with BioEdit software and screened

against the GenBank database using BLASTn tool of the NCBI site (http://www.ncbi.nlm.nih.gov/).

Minimal inhibitory concentrations (MIC) for Hg were determined for each isolated strains. Microtitration plates (96 wells) were prepared using two-fold dilutions of Hg in YPD liquid medium, from a starting concentration of 256 µM down to 0 µM. Growth was measured by spectrophotometry at DO_{595} after 24h and 48h of incubation at 25°C.

Results

Illumina MiSeq sequencing revealed high diversity of the leaf microbiome

Following total genomic DNA extraction from soil and poplar samples, amplicons of the ITS1 region were generated, and a total of 8,345,173 paired-end reads were obtained through Illumina MiSeq sequencing (Table S1). Among the 24 samples from each habitat, those exhibiting a low sequence count were eliminated from the rest of the analysis. Thus, a total of 7,519,254 filtered and non-chimeric fungal sequences constituted our final processed dataset, representing 90% of the initial post-sequencing reads, spread among 6,100 non-singleton OTUs defined by representative DNA sequences with sizes of 101 to 363 bp (mean = 181.9 bp). After subsampling, our dataset contained 26,672 reads per sample, distributed in 5,565 non-singletons OTUs.

Rarefaction curve analysis, which assesses OTUs richness as a result of sampling, showed that all samples approached an asymptote, revealing that the overall fungal diversity was well represented (Fig. S1). Moreover, the measured Good's coverage values (an estimator of completeness of sampling) were greater than 99% for each sample type (Table S1) and in every sample, highlighting good overall sampling. Coverage, richness, and diversity, estimates were

calculated for each dataset (Table 1). The Chao1 estimator of Mothur, indicated good sample OTUs richness throughout. The Shannon and Simpson diversity indices, measurements of overall diversity, indicated a diverse microbiota. More specifically, the diversity and richness estimates were always significantly higher in the soil samples, followed by the leaf, stem and root samples (Table 1).

A permutation test confirmed that the habitat ($R^2 = 0.58$) explained most of the variance in the fungal community, whereas variations between plots were negligible and not statistically significant (Table S2). The importance of the habitat factor was further corroborated through visualization in a NMDS plot (Fig. 1), and significant dissimilarity between all habitats was confirmed with the ANOSIM test (Table S3). The Bray-Curtis method indicated that the belowground and aboveground communities at the Tavaux site were well separated (Fig. 1a). Considering the global analysis, NMDS plots revealed that root samples exhibited the greatest between-sample variation (Fig. 1a). Furthermore, we showed that stem and leaf samples clustered closely together (Fig. 1a), although the NMDS plot of the belowground (Fig. 1b) or aboveground (Fig. 1c) communities alone showed a net clustering of each sample type in these two communities. The leaf data presented less scattering than the stem data (see sizes of ellipses in Fig. 1c). Overall, these data indicated higher homogeneity of the OTUs distribution in aboveground samples, while the soil and root samples were less homogeneous.

In the Venn diagram analysis, the sums of the total observed fungal OTUs in the four sampled habitats of the Skado plots were 1567, 609, 918 and 948 for the soil, root, stem and leaf samples, respectively (Fig. 2). Overall, 151 OTUs (5.9%) were shared by all habitats. The OTUs that were unique represented 52% and 35% of the belowground and aboveground samples, respectively (Fig. 2). The soil samples exhibited the highest proportion of unique OTUs (36.6%), followed by the leaf (10.2%) and stem (10.4%) samples. Conversely, the root samples shared > 97% of OTUs with another habitat, mostly with the soil habitat (>84.7% of

288 the root OTUs were detected in soil samples). Our data also revealed that in the poplar
289 phyllosphere, 51% of OTUs were shared by the stem and leaf samples, whereas 31% of OTUs
290 were shared by the soil and root samples.

291 ***Symbiotic fungi dominated the belowground habitats, whereas yeast-like fungi dominated***
292 ***the aboveground habitats***

293 The fungal communities across all four habitats were dominated by the phylum
294 *Ascomycota* (54.6% of total relative abundance on average), while *Basidiomycota* represented
295 a smaller portion of the communities (23.5%) (Fig. 3). However, the
296 *Ascomycota*/*Basidiomycota* ratios were significantly higher in the aboveground samples than
297 the belowground samples (Kruskal-Wallis $X^2 = 36.7$; $P < 1.4 \times 10^{-9}$). The largest proportion of
298 *Basidiomycota* was found in the root samples (Kruskal-Wallis $X^2 = 56.1$; $P < 4.0 \times 10^{-12}$). These
299 ratios are very similar to those identified with 454 sequencing technology in fungal
300 communities associated with broadleaf trees [42]. Few members of the known arbuscular
301 mycorrhizal fungi (AMF) phylum *Glomeromycota* were detected in the soil (0.25%, 92 OTUs
302 from the *Entrophospora* and *Rhizophagus* genera) and root (1.30%, 90 OTUs from the
303 *Entrophospora* and *Rhizophagus* genera) samples collected under poplars. OTUs assigned to
304 mycorrhizal species were virtually absent from all aboveground samples. Members of the
305 *Zygomycota* phylum were almost exclusively found in soil samples (5.2%, for 65 OTUs),
306 mostly associated to *Mortierella* species.

307 Across all samples, we detected a total of 21 distinct fungal classes, which were
308 unequally distributed, suggesting substantial differences between sampled habitats (Fig. 4). The
309 belowground habitats were enriched with *Agaricomycetes* (Kruskal-Wallis $X^2 = 69.8$; $P < 2.2 \times$
310 10^{-16}), *Pezizomycetes* (Kruskal-Wallis $X^2 = 69.5$; $P < 2.2 \times 10^{-16}$) and *Sordariomycetes* (Kruskal-
311 Wallis $X^2 = 67.9$; P< × 2.2 10^{-16}). Moreover, the root samples contained significantly more
312 *Agaricomycetes* (Kruskal-Wallis $X^2 = 16.3$; $P <$ × 5.4 10^{-5}), *Pezizomycetes* (Kruskal-Wallis $X^2 =$

313 25.4; $P < \times 4.6\ 10^{-7}$) and *Glomeromycetes* (Kruskal-Wallis $X^2 = 17.6$; $P < \times 2.8\ 10^{-5}$) but
314 significantly less Sordariomycetes and *Zygomycetes* than the soil samples. The aboveground
315 habitats were enriched in *Dothideomycetes* (Kruskal-Wallis $X^2 = 65.7$; $P < 5.4 \times 10^{-16}$) and
316 *Taphrinomycetes* (Kruskal-Wallis $X^2 = 69.8$; $P < 2.2 \times 10^{-16}$) from the *Ascomycota* phylum.
317 While some *Dothideomycetes* members were detected in root and soil samples,
318 *Taphrinomycetes* were virtually absent from all belowground samples. Although stem and leaf
319 sample habitats contained members of *Basidiomycota* classes, belonging to
320 *Agaricostillbomycetes* (Kruskal-Wallis $X^2 = 69.8$; $P < 2.2 \times 10^{-16}$), *Exobasidiomycetes* (Kruskal-
321 Wallis $X^2 = 69.8$; $P < 2.2 \times 10^{-16}$), *Microbotryomycetes* (Kruskal-Wallis $X^2 = 69.7$; $P < 2.2 \times 10^{-16}$)
322 and *Tremellomycetes* (Kruskal-Wallis $X^2 = 69.0$; $P < 2.2 \times 10^{-16}$), these classes were virtually
323 absent from all belowground samples. The high proportion of classes of unassigned fungi in the
324 stem habitat (63.5%) highlights the need for additional investigations of the diversity of the
325 fungi living in this particular habitat.

326 The assignment tools revealed that root and soil habitats were dominated by OTUs
327 identified as *Hymenogaster griseus, Thelephoraceae* and *Hebeloma hiemale*, all of which
328 belong to *Agaricomycetes* from the *Basidiomycota* phylum (Figs. 3 and 5). However, *Hebeloma*
329 (Kruskal-Wallis $X^2 = 8.7$; $P < \times 10^{-10}0.003$) and *Thelephoraceae* (Kruskal-Wallis $X^2 = 48.5$; $P <$
330 1.7×10^{-10}) OTUs dominated the root samples (Figs. 3 and 5), whereas *Hymenogaster* OTUs
331 (Kruskal-Wallis $X^2 = 4.3$; $P < 0.04^{-10}$) were the most abundant in soil samples (Fig. 3 and Fig.
332 5). By contrast, the aboveground samples were dominated by *Ascomycota* OTUs, mostly
333 belonging to 9 genera (*Alternaria*, *Aureobasidium*, *Bensigtonia, Lalaria, Davidiella,*
334 *Sphaerulina, Rhodotorula, Cryptococcus, Taphrina)*. The *Lalaria* (Kruskal-Wallis $X^2 = 29$; $P <$
335 1.7×10^{-8}) and *Davidiella* (Kruskal-Wallis $X^2 = 33$; $P < 9.2 \times 10^{-9}$) genera were most abundantly
336 found in leaves while a Pleosporale OTU was the most abundant in stems (Kruskal-Wallis

337 X^2=3.5; $P < 0.05$) (Fig. 3). The *Basidiomycota* OTUs in aboveground samples were mostly
338 assigned to the species *Bensigtonia yuccicola* (Figs. 3 and 5).

339 Each fungal OTU was further assigned to functional or morphological groups of fungi
340 using FUNguild (http://www.stbates.org/guilds/app.php) [43] (Fig. 6). For every assignment,
341 the FUNguild tool provides a confidence ranking, while referring to previously peer reviewed
342 data (Table S4). To examine the distribution of OTUs within the functional categories, the
343 abundance of the various OTU groups was set to 100%, and the OTUs were classified into
344 guilds (Fig. 6A) and morphological categories (Fig. 6B). The investigation of trophic status in
345 the belowground habitats revealed dominance of symbiotrophs in the root habitat (70.5%),
346 while the soil community was composed of saprotrophs (45%), symbiotrophs (40%) and
347 biotrophs (14%). In the aboveground habitats, saprotrophic fungi appeared to be dominant
348 (stem, 53%; leaf, 65%) (Fig. 6a). The symbiotrophic fungi identified in the aboveground
349 habitats belong mostly to the lichenized genus *Sphaerulina,* whereas symbiotrophs from the
350 belowground habitats were identified as ectomycorrhizal fungi from the *Hymenogaster* genus.
351 Another dichotomy was clearly revealed between the belowground and aboveground habitats
352 through the analysis of growth form morphology (Fig. 6b). Indeed, as the soil and root habitats
353 were dominated by gasteroid (soil: 67%; root: 48%) and agaricoid (soil: 21%; root: 45%) fungi,
354 the fungal communities from the stem and leaf habitats were essentially dominated by yeasts
355 (stem: 4%; leaf: 11%), dimorphic yeasts (stem: 62%; leaf: 38%), thallus fungi (stem: 27%; leaf:
356 1%) or rot fungi (stem: 11%; leaf: 37%). The presence of basidiomycetous or ascomycetous
357 yeast in the phyllosphere has previously been observed in plants from temperate, tropical and
358 Mediterranean climates [44, 45], in agreement with our results.

359 ***Interactions with Hg***

360 The analysis of Hg in the various matrices revealed that the belowground habitats
361 contained 100 times more Hg compared with the aboveground habitats (Fig. S2). In detail, the
362 average values of Hg were 42.5 ng/g DM in poplar leaves and 3.6 ng/g DM in poplar stems,
363 which are within the range of previously published data [21]. The root samples exhibited Hg
364 concentrations of approximately 2.4 µg/g of DM. The soils exhibited an average Hg
365 concentration of 5.6 µg/g DM, in agreement with our previous data [13], but ranged from 2.92
366 to 9.08 µg/g DM within the various harvested soil samples. Given the large variations in Hg
367 concentrations in each habitat, we analyzed the correlations with Hg concentrations in the
368 various matrices and found that only soil samples showed significant correlations between the
369 Hg concentration and the diversity or richness indices. Specifically, we found a significant
370 negative correlation between the soil Hg content and fungal richness indices (Observed
371 richness: Spearman correlation coefficient of $r^2 = -0.68$ and $p < 0.001$; Chao1 index: Spearman
372 correlation coefficient of $r^2 = -0.42$, and $p < 0.05$). The abundance of the two fungal classes,
373 *Eurotiomycetes* ($r^2 = 0.63$, and $p < 0.001$) and *Sordariomycetes* ($r^2 = 0.41$, $p < 0.05$), were
374 correlated with soil Hg concentrations, as well as the abundance of the two following OTUs,
375 corresponding to a *Thelephoraceae* ($r^2 = 0.44$, and $p < 0.05$) and a *Trichoderma* ($r^2 = 0.48$, and
376 $p < 0.05$) species. Conversely, the abundance of an OTU identified as *Hymenogaster griseus*
377 was significantly negatively correlated with Hg ($r^2 = -0.46$, and $p < 0.05$). None of the diversity,
378 richness or abundance indices were significantly correlated in root, leaf or stem with the Hg
379 concentrations (data not shown).

380 The number of yeast cells isolated from the phyllosphere was $2.5.10^7$ UFC/ml without
381 Hg but decreased to $1.9.10^7$ UFC/ml, $1.2.10^6$ UFC/ml, 1.10^6 UFC/ml and 2.10^5 UFC/ml on
382 media enriched with 2, 5, 10 or 20 µM of $HgCl_2$, respectively. At 10 µM $HgCl_2$, only 2 species
383 were isolated, namely *Nakazawaea populi* formely known as *Candida populi,* and
384 *Aureobasidium pullulans,* which was one of the most abundant OTU (2.5 % of detected

sequences) of the metabarcoding dataset obtained from the leaf habitat. The MIC values for Hg of the isolated strains were 32 µM for *Nakazawaea populi* and 16 µM for *Aureobasidium pullulans* (Table 2).

The co-occurrence network revealed rare fungal OTUs with a high level of interaction in the community

We built co-occurrence networks to further assess the links within the fungal communities of the four habitats (Fig. 8 and Table 3). After network calculations, some topological properties that are commonly used in network analysis were completed to reveal complex patterns [46]. The root and soil habitats harbored the highest network connectivity, as exemplified by the highest number of edges and nodes (Fig. 8, Table 3). The co-presence and mutual exclusion of OTUs in the whole dataset were equally well distributed in the leaf, stem and root, habitats, whereas soil showing the highest mutual exclusion percentage (Table 3).

The network indices allowed us to define the 10 dominant keystone OTUs for each habitat (Table S5), which were defined as being important to maintain the function and structure of the microbial community and were arbitrarily identified here based on the number of connections established with the rest of the network [47]. Some taxa can be less abundant but highly connected with other taxa (as shown by the number of degrees within the node). These keystone OTUs can be divided in two groups: those generating positive connections (co-presence) and those generating negative connections (mutual exclusion). Both (+ and -) groups were evident in this subset of keystone OTUs in the leaf, stem and root habitats, whereas the soil contained mostly OTUs exhibiting negative connections, as observed for the whole soil dataset. The tendency of OTUs to cluster is revealed by the clustering coefficient, which was two-fold higher for the root habitat. In the leaf habitat, OTUs from the genus *Myrothecium* and from the class *Dothideomycetes* (unassigned genus) produced the highest number of negative

409 connections. The genus *Myrothecium*, previously detected in mulberry, has been identified as
410 a foliar pathogen producing mycotoxins [48]. Our work revealed that OTUs from this genus
411 found on poplar leaves had an overall negative impact on other microbes from the leaf
412 community. In the stem habitat, an OTU from the *Exobasidiomycetes* class showed only
413 negative connections with all other fungal OTUs. The other keystone OTUs from the stem
414 belonged to the *Dothideomycetes* class and exhibited mostly negative connections. Similarly,
415 in the root habitat, two keystone OTUs belonging to *Glomeromycetes* exhibited mostly negative
416 connections with other OTUs. In contrast to the leaf and stem habitats, other keystone OTUs
417 presented mostly positive connections, constituting a cluster highlighted in Figure 8.
418 *Rhodotorula* and *Lalaria* OTUs from this cluster were rather rare in the root habitat but were
419 frequently encountered in the leaf habitat (Fig. 3). The soil habitat was characterized by
420 keystone OTUs exhibiting mostly negative connections. The *Peziza* OTU (ITS-75-68665)
421 displayed the greatest number of connections among all keystone OTUs by far (Table S5).

422

423 **Discussion**

424 We used the Illumina MiSeq sequencing platform to characterize fungal communities
425 from a poplar plantation at a Hg-contaminated site. It is important to bear in mind that we were
426 unable to distinguish between endophytes and epiphytes in each of the three plant habitats (root,
427 stem and leaf) and instead considered the fungal communities in these habitats in their entirety.
428 Although we did not set out to study seasonal dynamics of the belowground and aboveground
429 fungal communities, we should bear in mind that differing seasonal patterns between
430 belowground [49] and aboveground [50, 51] fungal taxa have been described previously. It was
431 concluded that the variation of foliar chemistry across growing seasons should not be
432 considered a major driver of the observed fungal dynamics.

Rarefaction analyses and richness estimators indicate that much of the total diversity detectable with the Illumina-based sequencing was obtained. The finding of higher richness and diversity in aboveground habitats compared with the root habitat was poorly predictable, as there are considerably fewer available studies on aboveground communities, compared with belowground communities. A previous study revealed a low percentage of fungal OTUs shared by leaf and root samples in *Fagus sylvatica* trees [42], while another study showed that a majority of aboveground OTUs were also present in the belowground compartment of agave plants [3]. Our dataset unequivocally revealed that i) less than 6% of the OTUs were detected in all four habitats, and ii) the aboveground fungal communities from poplar leaves were extremely diverse, although they were represented by only a few abundant taxa and numerous rare taxa [15, 52]. Overall, our results strongly indicate that belowground habitats host fungal communities almost completely isolated from from the aboveground habitats communities in terms of taxonomy, growth morphology, and relationship with trees or microbial interactions. Considering previous studies, the finding of lower richness and diversity in the root compared with the soil habitat was expected [3, 11, 53]. Clear separation of microbiomes has been reported for soil and root samples from mature poplars [54] and 2-year-old poplars [11]. In our study, we showed that 87% of the detectable OTUs of the roots habitat were also found in the soil habitat but few taxa were strongly associated to root. Thus, the root fungal communities also displayed lower homogeneity of the species distribution compared with soil communities.

We demonstrated that the fungal communities associated with *Populus* roots mostly consisted of ectomycorrhizal fungi, which are known to develop mutually beneficial interactions with their hosts. These plant-microorganism interactions in the root compartment are probably one of the factors explaining the reasonable adaptation of *Populus skado* to this particular soil. The *Thelephorales* OTUs in the root samples accounted for the main contribution to the dominance of symbiotrophs in roots, as most members of this order are

458 known to be ectomycorrhizal and to live in symbiosis with various host plants across Northern
459 America and Europe. *Thelephoraceae* are indeed abundant colonizers of *Salix caprea* or
460 *Populus tremula* roots in TE-contaminated soils [55–57]. Additionally, OTUs corresponding to
461 the *Hebeloma*, *Cortinarius* and *Geopora* genera were also detected in our root and soil samples,
462 in agreement with previous studies [55, 56]. Members of the *Hebeloma* mycorrhizal genus
463 (notably *H. mesophaeum*) are frequently found within unvegetated soils [55, 56] and have been
464 shown to promote the growth of host trees in soils contaminated with metals [58]. At the family
465 level, both this and a previous study by our group [13] identified *Agaricomycetes* and
466 *Pezizomycetes* as the most frequent fungal families in the belowground compartment. Similarly,
467 five of the 6 most common genera (*Hebeloma, Mortierella, Tuber, Geopora* and *Cortinarius*,
468 but not *Hymenogaster*) identified in this study were among the top five detected previously.

469 The analysis of growth morphology clearly resulted in clustering of the belowground
470 and aboveground habitats. The soil and root habitats were dominated by agaricoid and gasteroid
471 fungi, as highlighted by the presence of *Hebeloma* and *Hymenogaster* species, respectively.
472 The fungi from stem and leaf communities were essentially identified as yeasts or facultative
473 yeast morphotypes (Fig. 6b), as exemplified by *Lalaria* OTUs [59]. Abundance of *Lalaria*
474 OTUs in the phyllosphere has previously been reported on the leaves of *Fagus sylvatica* [60]
475 and in the *Quercus* phyllosphere [15]. *Davidiella tassiana*, also known as *Mycosphaerella*
476 *tassiana* or *Cladosporium herbarum*, is a leaf pathogenic fungus from the Helotiales order that
477 is commonly encountered in the phyllosphere of trees [61]. Reader should keep in mind that
478 many fungi have several names, which can lead to mistakes and thus have always to be taken
479 in consideration when using dated data. Standardization at a global scale of fungal names should
480 only profit to fungal ecology. The stem tissues were enriched in *Pleosporales sp. and*
481 *Sphaerulina pseudovirgaureae* OTUs. Previous studies have shown that phyllosphere

endophytic fungi can play an important role in enhancing plant health [20], acting as biocontrol agents against other plants, insects and pathogens.

Hg is known to be a toxic element, but only few studies have explored the impact of Hg on fungal communities in field trials. Müller (2001) showed that the soil fungal biomass was not affected by the Hg along a Hg gradient ranging from 7-522 mg THg/kg of soil. Over a narrow gradient in terms of the Hg concentration, only a negative correlation between arbuscular mycorrhizal fungi and Hg was observed in the literature, while no correlation was found between ectomycorrhizal (ECM) fungi and Hg [63]. Therefore, this study is the first to describe a significant negative effect of Hg on soil fungal richness and diversity under long-term, natural Hg exposure. In contrast, Hg exposure was not a major driver of the root, stem and leaf communities, probably due to the limited variations and the limited impact these variations may have on cellular processes. Nevertheless, we were able to isolate some Hg resistant yeast strains from the leaf habitat. Resistance here refer to the fact that these strains were isolated on Hg-enriched growth media, and to the MIC measured for these strains, which are comparable to previously published data [64]. As most of the Hg detected in poplar leaves entered through the atmospheric pathway [21], we indeed focused on the isolation of Hg resistant fungi from this habitat. We thus isolated *Aureobasidium pullulans* Hg resistant strains, also highly represented in the leaf metabarcoding dataset (Fig. 3). This species is recognized as an active phylloplane colonizer [65], which showed some capacity to bind metals to the cell surfaces [66]. Other, authors previously revealed that melanized fungi such as *Aureobasidium pullulans*, *Cladosporium spp.* and *Alternaria alternate* have been isolated from soil samples treated with toxic industrial wastes containing high concentrations of copper and mercury and may also be dominant members of the mycobiota of metal-contaminated phylloplanes [67]. We also isolated *Nakazawaea populi* Hg resistant strains, that were not detected in our metabarcoding dataset, probably due to an uncomplete

assignment, and that may be part of the unassigned *Ascomycota* cluster (Fig. 3). This strain has been recently assigned to the *Nakazawaea* genus, and was previously known as a member of the *Candida* genus [68]. *C. populi* was indeed isolated from poplar sap exudate [69]. These strains will be further used in inoculation experiments, to better understand the role of leaf yeast communities on the overall Hg cycle between soil, atmospheric and leaf compartments.

This study is the first to explore the organization of the fungal communities of soil, roots, stems and leaves using a co-occurrence approach at the scale of a clonal tree stand. Indeed, previous studies have focused on species abundance and diversity, but not on the interactions among species, which could be more important to ecosystem functioning [70]. Co-occurrence networks represent individual microbes (operational taxonomic units (OTUs)) as nodes and feature–feature pairs as edges, where an edge may imply a biologically or biochemically meaningful relationship between features, and are based on correlations [34]. For instance, one may expect that mutualistic microbes, or those that benefit each other, will co-occur across samples. In contrast, antagonistic relationships between microbes, such as competition for the same niche, result in a mutual exclusion. It has been observed that phylogenetically related microbes have a tendency to positively co-occur [71]. In practice, microbes may exhibit positive or negative correlations for indirect reasons, based on their environmental preferences. The overall dataset revealed that non-abundant OTUs might play a significant role in the network of interactions. Co-occurrence network analysis of the fungal communities from the four habitats established a clear dichotomy between soil and the three other habitats, where the soil community was dominated by negative edges, known as mutual exclusion. It should be noted that sequencing depth impacts the percentage of positive edges in the network, with a low depth resulting in spurious positive correlations [37]. Thus, the large number of negative correlations found in our study can be correlated with our extremely high sequencing depth. This dominance of negative degrees found in the soil (80%), but not in the

roots nor in the aboveground habitats, could reflect a high degree of competition between fungi in the soil due to a lack of nutrient availability in the absence of tree exudates. It is also possible that the soil microorganisms under the canopy were in competition with the plants for nutrients such as nitrogen, exacerbating the nutrient competition between microorganisms [72]. The network obtained from the fungal sequencing data also revealed that the root compartment present the highest number of interactions between fungi and the highest clustering coefficient, with predominance of *Glomeromycetes*, showing a great number of interactions with other fungi. Arbuscular mycorrhizas (AM) formed by *Glomeromycetes* are widespread in living plants, supporting the ancestral origin of the plant–*Glomeromycetes* symbiosis, as fully supported by the literature [73]. We noted that the class *Glomeromycetes* produced many degrees of mutual exclusion with other classes and between the most interactive *Glomeromycetes* themselves. The hub in the root compartment network typical of the leaf compartment could correspond to the transfer of microorganisms during leaf fall in the root area, but the real explanation is still unclear.

We may conclude that each habitat that we studied represents a unique niche for the fungal communities in a monoclonal plantation of the cultivar Skado (*P. trichocarpa* x *P. maximowiczii*) implemented in 2011 as a short-rotation coppice (SRC, 2200 stems/ha). Aboveground and belowground poplar habitats host completely different fungal communities, as highlighted by the core microbiome of the four habitats that represent only reduced to 5.9% of the total OTUs. We will further explore the role of fungal organisms in the Hg cycle, which deserves attention. We believe that our findings will be instructive for the design of future ecological restoration practices.

Acknowledgments

556 This work was supported by the French National Research Agency [ANR BIOFILTREE
557 2010-INTB-1703-01], the ADEME (French Environment and Energy Management Agency)
558 [PROLIPHYT 1172C0053], the Région Franche-Comté [Environnement-Homme-Territoire
559 2014-069], the Pays de Montbéliard Agglomération [13/070-203-2015], and the French
560 national program EC2CO- MicrobiEen FREIDI-Hg. A.D. received a PhD grant from the
561 Région Franche-Comté.

562 A.D and F.M. contributed equally to this work.

563

564

565 **References**

566 1. van der Heijden MGA, Hartmann M (2016) Networking in the Plant Microbiome. PLOS Biol
567 14:e1002378. doi: 10.1371/journal.pbio.1002378

568 2. Leff JW, Tredici P Del, Friedman WE, Fierer N (2014) Spatial structuring of bacterial
569 communities within individual Ginkgo biloba trees. Environ Microbiol 17:2352–2361. doi:
570 10.1111/1462-2920.12695

571 3. Coleman-Derr D, Desgarennes D, Fonseca-Garcia C, et al (2015) Biogeography and cultivation
572 affect microbiome composition in the drought-adapted plant Subgenus Agave. New Phytol
573 209:798–811. doi: 10.1111/nph.13697

574 4. Balint M, Bartha L, O'Hara RB, et al (2015) Relocation, high-latitude warming and host
575 genetic identity shape the foliar fungal microbiome of poplars. Mol Ecol 24:235–248. doi:
576 10.1111/mec.13018

577 5. Lenoir I, Fontaine J, Lounès-Hadj Sahraoui A (2016) Arbuscular mycorrhizal fungal responses
578 to abiotic stresses: A review. Phytochemistry 123:4–15. doi: 10.1016/j.phytochem.2016.01.002

579 6. Whipps JM, Hand P, Pink D, Bending GD (2008) Phyllosphere microbiology with special
580 reference to diversity and plant genotype. J Appl Microbiol 105:1744–55. doi: 10.1111/j.1365-
581 2672.2008.03906.x

582 7. Ritpitakphong U, Falquet L, Vimoltust A, et al (2016) The microbiome of the leaf surface of
583 Arabidopsis protects against a fungal pathogen. New Phytol 210:1033–1043. doi:
584 10.1111/nph.13808

585 8. Waller F, Achatz B, Baltruschat H, et al (2005) The endophytic fungus Piriformospora indica
586 reprograms barley to salt-stress tolerance, disease resistance, and higher yield. Proc Natl Acad
587 Sci U S A 102:13386–13391. doi: 10.1073/pnas.0504423102

588 9. Hartley SE, Gange AC (2009) Impacts of plant symbiotic fungi on insect herbivores:

589 mutualism in a multitrophic context. Annu Rev Entomol 54:323–42. doi:
590 10.1146/annurev.ento.54.110807.090614

591 10. Martínez-Álvarez P, Fernández-González RA, Sanz-Ros AV, et al (2016) Two fungal
592 endophytes reduce the severity of pitch canker disease in Pinus radiata seedlings. Biol Control
593 94:1–10. doi: 10.1016/j.biocontrol.2015.11.011

594 11. Danielsen L, Thürmer A, Meinicke P, et al (2012) Fungal soil communities in a young
595 transgenic poplar plantation form a rich reservoir for fungal root communities. Ecol Evol
596 2:1935–1948. doi: 10.1002/ece3.305

597 12. Tedersoo L, Bahammad B, Polme S, et al (2014) Global diversity and geography of soil fungi.
598 Science (80-) 346:1256688.

599 13. Zappelini C, Karimi B, Foulon J, et al (2015) Diversity and complexity of microbial
600 communities from a chlor-alkali tailings dump. Soil Biol Biochem 90:101–110. doi:
601 10.1016/j.soilbio.2015.08.008

602 14. Yergeau E, Lawrence JR, Sanschagrin S, et al (2012) Next-generation sequencing of microbial
603 communities in the athabasca river and its tributaries in relation to oil sands mining activities.
604 Appl Environ Microbiol 78:7626–7637. doi: 10.1128/AEM.02036-12

605 15. Jumpponen A, Jones KL (2009) Massively parallel 454 sequencing indicates hyperdiverse
606 fungal communities in temperate Quercus macrocarpa phyllosphere. New Phytol 184:438–448.
607 doi: 10.1111/j.1469-8137.2009.02990.x

608 16. Knief C, Delmotte N, Chaffron S, et al (2012) Metaproteogenomic analysis of microbial
609 communities in the phyllosphere and rhizosphere of rice. ISME J 6:1378–1390. doi:
610 10.1038/ismej.2011.192

611 17. Bonito G, Reynolds H, Robeson MS, et al (2014) Plant host and soil origin influence fungal
612 and bacterial assemblages in the roots of woody plants. Mol Ecol 23:3356–70. doi:
613 10.1111/mec.12821

614 18. Foulon J, Zappelini C, Durand A, et al (2016) Impact of poplar-based phytomanagement on
615 soil properties and microbial communities in a metal-contaminated site. FEMS Microbiol Ecol
616 92:fiw163. doi: 10.1093/femsec/fiw163

617 19. Faust K, Sathirapongsasuti JF, Izard J, et al (2012) Microbial co-occurrence relationships in the
618 Human Microbiome. PLoS Comput Biol 8:e1002606. doi: 10.1371/journal.pcbi.1002606

619 20. Xiang L, Gong S, Yang L, et al (2015) Biocontrol potential of endophytic fungi in medicinal
620 plants from Wuhan Botanical Garden in China. Biol Control 94:47–55. doi:
621 10.1016/j.biocontrol.2015.12.002

622 21. Assad M, Parelle J, Cazaux D, et al (2015) Mercury uptake into poplar leaves. Chemoshpere
623 146:1–7. doi: 10.1016/j.chemosphere.2015.11.103

624 22. Hacquard S, Schadt CW (2015) Towards a holistic understanding of the beneficial interactions
625 across the Populus microbiome. New Phytol 205:1424–30. doi: 10.1111/nph.13133

626 23. Maillard F, Girardclos O, Assad M, et al (2016) Dendrochemical assessment of mercury
627 releases from a pond and dredged-sediment landfill impacted by a chlor-alkali plant. Environ
628 Res 148:122–126. doi: 10.1016/j.envres.2016.03.034

629 24. Lefort F, Douglas GC (1999) An efficient micro-method of DNA isolation from mature leaves
630 of four hardwood tree species Acer, Fraxinus, Prunus and Quercus. Ann For Sci 56:259–263.
631 doi: 10.1051/forest:19990308

632 25. Healey A, Furtado A, Cooper T, Henry RJ (2014) Protocol: a simple method for extracting
633 next-generation sequencing quality genomic DNA from recalcitrant plant species. Plant
634 Methods 10:21. doi: 10.1186/1746-4811-10-21

635 26. Huang CL, Jian FY, Huang HJ, et al (2014) Deciphering mycorrhizal fungi in cultivated
636 Phalaenopsis microbiome with next-generation sequencing of multiple barcodes. Fungal Divers
637 66:77–88. doi: 10.1007/s13225-014-0281-x

638 27. Smith DP, Peay KG (2014) Sequence depth, not PCR replication, improves ecological
639 inference from next generation DNA sequencing. PLoS One 9:e90234. doi:
640 10.1371/journal.pone.0090234

641 28. Gweon HS, Oliver A, Taylor J, et al (2015) PIPITS: An automated pipeline for analyses of
642 fungal ITS sequences from the Illumina sequencing platform. Methods Ecol Evol 6:973–980.
643 doi: 10.1111/2041-210X.12399

644 29. Dickie IA (2010) Insidious effects of sequencing errors on perceived diversity in molecular
645 surveys. New Phytol 188:916–918. doi: 10.1111/j.1469-8137.2010.03473.x

646 30. Tedersoo L, May TW, Smith ME (2010) Ectomycorrhizal lifestyle in fungi: global diversity,
647 distribution, and evolution of phylogenetic lineages. Mycorrhiza 20:217–263. doi:
648 10.1007/s00572-009-0274-x

649 31. Kõljalg U, Nilsson RH, Abarenkov K, et al (2013) Towards a unified paradigm for sequence-
650 based identification of fungi. Mol Ecol 22:5271–5277. doi: 10.1111/mec.12481

651 32. Schloss PD, Westcott SL, Ryabin T, et al (2009) Introducing mothur: Open-Source, Platform-
652 Independent, Community-Supported Software for Describing and Comparing Microbial
653 Communities. Appl Environ Microbiol 75:7537–7541. doi: 10.1128/AEM.01541-09

654 33. Bell TH, El-Din Hassan S, Lauron-Moreau A, et al (2014) Linkage between bacterial and
655 fungal rhizosphere communities in hydrocarbon-contaminated soils is related to plant
656 phylogeny. ISME J 8:331–43. doi: 10.1038/ismej.2013.149

657 34. Weiss S, Van Treuren W, Lozupone C, et al (2016) Correlation detection strategies in
658 microbial data sets vary widely in sensitivity and precision. ISME J. doi:
659 10.1038/ismej.2015.235

660 35. Faust K, Raes J (2012) Microbial interactions: from networks to models. Nat Rev Microbiol
661 10:538–550. doi: 10.1038/nrmicro2832

662 36. Christmas R, Avila-Campillo I, Bolouri H, et al (2005) Cytoscape: a software environment for
663 integrated models of biomolecular interaction networks. Am Assoc Cancer Res Educ B
664 13:2498–2504. doi: 10.1101/gr.1239303.metabolite

665 37. Faust K, Lima-Mendez G, Lerat JS, et al (2015) Cross-biome comparison of microbial
666 association networks. Front Microbiol 6:1–13. doi: 10.3389/fmicb.2015.01200

667 38. Berry D, Widder S (2014) Deciphering microbial interactions and detecting keystone species
668 with co-occurrence networks. Front Microbiol 5:1–14. doi: 10.3389/fmicb.2014.00219

669 39. Samczyński Z, Dybczyński RS, Polkowska-Motrenko H, et al (2012) Two new reference
670 materials based on tobacco leaves: certification for over a dozen of toxic and essential
671 elements. ScientificWorldJournal 2012:216380. doi: 10.1100/2012/216380

672 40. Fu S-F, Sun P-F, Lu H-Y, et al (2016) Plant Growth–Promoting Traits of Yeasts Isolated from
673 the Phyllosphere and Rhizosphere of Drosera spathulata Lab. Fungal Biol 120:433–448. doi:
674 10.1016/j.funbio.2015.12.006

675 41. Sun PF, Fang WT, Shin LY, et al (2014) Indole-3-Acetic Acid-Producing Yeasts in the
676 Phyllosphere of the Carnivorous Plant. 1–22. doi: 10.1371/journal.pone.0114196

677 42. Coince A, Cordier T, Lengellé J, et al (2014) Leaf and root-associated fungal assemblages do
678 not follow similar elevational diversity patterns. PLoS One 9:e100668. doi:
679 10.1371/journal.pone.0100668

680 43. Nguyen NH, Song Z, Bates ST, et al (2015) FUNGuild: An open annotation tool for parsing
681 fungal community datasets by ecological guild. Fungal Ecol 20:241–248. doi:
682 10.1016/j.funeco.2015.06.006

683 44. Inacio J, Portugal L, Spencer-Martins I, Fonseca A (2005) Phylloplane yeasts from Portugal:
684 Seven novel anamorphic species in the Tremellales lineage of the Hymenomycetes
685 (Basidiomycota) producing orange-coloured colonies. FEMS Yeast Res 5:1167–1183. doi:
686 10.1016/j.femsyr.2005.05.007

687 45. Limtong S, Koowadjanakul N (2012) Yeasts from phylloplane and their capability to produce
688 indole-3-acetic acid. World J Microbiol Biotechnol 28:3323–3335. doi: 10.1007/s11274-012-
689 1144-9

690 46. Barberán A, Bates ST, Casamayor EO, Fierer N (2012) Using network analysis to explore co-
691 occurrence patterns in soil microbial communities. ISME J 6:343–351. doi:
692 10.1038/ismej.2011.119

693 47. Lupatini M, Suleiman AK a., Jacques RJS, et al (2014) Network topology reveals high
694 connectance levels and few key microbial genera within soils. Front Environ Sci 2:1–11. doi:
695 10.3389/fenvs.2014.00010

696 48. Murakami R, Kawakita H, Shirata A (2002) Infection behaviour of conidia of Myrothecium
697 roridum on mulberry leaf and cytological changes of leaf cells infected with the fungus.
698 Séricologia 42:19–38.

699 49. Shakya M, Gottel N, Castro H, et al (2013) A multifactor analysis of fungal and bacterial
700 community structure in the root microbiome of mature Populus deltoides trees. PLoS One
701 8:e76382. doi: 10.1371/journal.pone.0076382

702 50. Glushakova AM, Chernov IY (2004) Seasonal Dynamics in a Yeast Population on Leaves of
703 the Common Wood Sorrel Oxalis acetosella L . Microbiology 73:184–188. doi:
704 10.1023/B:MICI.0000023987.40253.2d

705 51. Jumpponen A, Jones KL (2010) Seasonally dynamic fungal communities in the Quercus
706 macrocarpa phyllosphere differ between urban and nonurban environments. New Phytol
707 186:496–513. doi: 10.1111/j.1469-8137.2010.03197.x

708 52. Balint M, Tiffin P, Hallstrom B, et al (2013) Host Genotype Shapes the Foliar Fungal
709 Microbiome of Balsam Poplar (Populus balsamifera). PLoS One 8:e53987. doi:
710 10.1371/journal.pone.0053987

711 53. Foulon J, Zappelini C, Durand A, et al (2016) Environmental metabarcoding reveals

712 contrasting microbial communities at two poplar phytomanagement sites. Sci Total Environ
713 571:1230–1240. doi: 10.1016/j.scitotenv.2016.07.151

714 54. Gottel NR, Castro HF, Kerley M, et al (2011) Distinct Microbial Communities within the
715 Endosphere and Rhizosphere of Populus deltoides Roots across Contrasting Soil Types. Appl
716 Environ Microbiol 77:5934–5944. doi: 10.1128/AEM.05255-11

717 55. Regvar M, Likar M, Piltaver A, et al (2010) Fungal community structure under goat willows
718 (Salix caprea L.) growing at metal polluted site: the potential of screening in a model
719 phytostabilisation study. Plant Soil 330:345–356. doi: 10.1007/s11104-009-0207-7

720 56. Krpata D, Peintner U, Langer I, et al (2008) Ectomycorrhizal communities associated with
721 Populus tremula growing on a heavy metal contaminated site. Mycol Res 112:1069–1079. doi:
722 10.1016/j.mycres.2008.02.004

723 57. Hrynkiewicz K, Haug I, Baum C (2008) Ectomycorrhizal community structure under willows
724 at former ore mining sites. Eur J Soil Biol 44:37–44. doi: 10.1016/j.ejsobi.2007.10.004

725 58. Hrynkiewicz K, Dabrowska G, Baum C, et al (2012) Interactive and Single Effects of
726 Ectomycorrhiza Formation and Bacillus cereus on Metallothionein MT1 Expression and
727 Phytoextraction of Cd and Zn by Willows. Water Air Soil Pollut 223:957–968. doi:
728 10.1007/s11270-011-0915-5

729 59. Inácio J, Rodrigues MG, Sobral P, Fonseca Á (2004) Characterisation and classification of
730 phylloplane yeasts from Portugal related to the genus Taphrina and description of five novel
731 Lalaria species. FEMS Yeast Res 4:541–555. doi: 10.1016/S1567-1356(03)00226-5

732 60. Cordier T, Stan, Robin C, et al (2012) The composition of phyllosphere fungal assemblages of
733 European beech (Fagus sylvatica) varies significantly along an elevation gradient. New Phytol
734 196:510–519.

735 61. Jakuschkin B, Fievet V, Schwaller L, et al (2016) Deciphering the Pathobiome: Intra- and
736 Interkingdom Interactions Involving the Pathogen Erysiphe alphitoides. Environ Microbiol 1–

11. doi: 10.1007/s00248-016-0777-x

62. Müller A (2001) The effect of long-term mercury pollution on the soil microbial community. FEMS Microbiol Ecol 36:11–19.

63. Jean-Philippe SR, Franklin JA, Buckley DS, Hughes K (2011) The effect of mercury on trees and their mycorrhizal fungi. Environ Pollut 159:2733–2739. doi: 10.1016/j.envpol.2011.05.017

64. Moller AK, Barkay T, Hansen M a., et al (2014) Mercuric reductase genes (merA) and mercury resistance plasmids in High Arctic snow, freshwater and sea-ice brine. FEMS Microbiol Ecol 87:52–63. doi: 10.1111/1574-6941.12189

65. Andrews JH, Harris RF (2000) The ecology and biogeography of microorganisms on plant surfaces.

66. Gadd geoffrey M, Mowll JL (1985) Copper uptake by yeast-like cells, Hyphae and chlamydospores of Aureobasidium pullulans. Exp Mycrobiology 9:230–240.

67. Gadd GM (2007) Geomycology: biogeochemical transformations of rocks, minerals, metals and radionuclides by fungi, bioweathering and bioremediation. Mycol Res 111:3–49. doi: 10.1016/j.mycres.2006.12.001

68. Kurtzman CP, Robnett CJ (2014) Description of Kuraishia piskuri f.a., sp. nov., a new methanol assimilating yeast and transfer of phylogenetically related Candida species to the genera Kuraishia and Nakazawaea as new combinations. FEMS Yeast Res 14:1028–1036. doi: 10.1111/1567-1364.12192

69. Hagler AN, Mendonca-Hagler LC, Phaff HJ (1989) Candida populi, a new species of yeast occurring in exudates of Populus and Betula species. Int J Syst Evol Microbiol 39:97–99. doi: 10.1099/00207713-39-2-97

70. Lu L, Yin S, Liu X, et al (2013) Fungal networks in yield-invigorating and -debilitating soils induced by prolonged potato monoculture. Soil Biol Biochem 65:186–194. doi:

761 10.1016/j.soilbio.2013.05.025

762 71. Lozupone C, Faust K, Raes J, et al (2012) Identifying genomic and metabolic features that can
763 underlie early successional and opportunistic lifestyles of human gut symbionts. Genome Res
764 22:1974–1984. doi: 10.1101/gr.138198.112

765 72. Kaye JP, Hart SC (1997) Competition for nitrogen between plants and soil microorganisms.
766 Trends Ecol Evol 12:139–143. doi: 10.1016/S0169-5347(97)01001-X

767 73. Selosse MA, Strullu-Derrien C, Martin FM, et al (2015) Plants, fungi and oomycetes: A 400-
768 million year affair that shapes the biosphere. New Phytol 206:501–506. doi:
769 10.1111/nph.13371

770

771

772

773

774 **Figure legends**

775

776 **Figure 1.** Non-parametric multidimensional scaling (NMDS) plot of fungal communities associated
777 with the four poplar habitats, using the Bray-Curtis dissimilarity measure. Each point represents the
778 fungal community of a given sample. Each color represents one of the 6 trees sampled. Confidence area
779 of ellipses = 0.95. (a) All habitats, (b) belowground habitats, and (c) aboveground habitats.

780 **Figure 2.** Venn diagram showing the overlap of the fungal communities from the four poplar habitats,
781 based on OTUs. OTU delineation was based on a threshold of < 97% sequence similarity

782 **Figure 3**. Proportion and taxonomic assignment of abundant and rare (< 0.5% relative abundance)
783 operational taxonomic units (OTUs) from the various poplar habitats. The assignments are given at the
784 lowest taxonomic level possible, with relative proportions presented in parentheses. The abundance of
785 the major phyla and the total number of reads are provided on the left side of each graph, color coded
786 as follows: *Ascomycota* (red), *Basidiomycota* (blue), *Zygomycota* (yellow), *Chytridiomycota* (brown),
787 *Glomeromycota* (green) and unassigned fungi (grey).

788 **Figure 4.** Composition of the fungal communities from the various poplar habitats at the class level.
789 The data were derived from MiSeq sequencing of the ITS1 region.

790 **Figure 5.** Heat map and hierarchical cluster analysis of the relative abundance of fungal OTUs from the
791 various poplar habitats. Letters indicate significantly different abundances at $p < 0.05$ (Kruskal-Wallis
792 comparison test), n=23 (root and leaf) or n=24 (soil and stem). The dendrogram represents linkage
793 clustering using Euclidean distance measures. OTU delineation was based on a threshold of < 97%
794 sequence similarity. The number associated with the OTU corresponds to the relative abundance rank
795 of that OTU in the total dataset. Assignments between brackets show the lowest taxonomic level
796 associated with the OTU using the UNITE database, k: kingdom, p: phylum, o: order, c: class, f: family,
797 s: genus_species.

Figure 6. Relative proportions of fungal sequences from the various poplar habitats assigned to major fungal guilds (a) and morphological groups (b).

Figure 7. Box plots of the Hg concentration (ng/mg DM) in (a) belowground habitats, and (b) aboveground habitats. Letters indicate significant differences between habitats (p-value < 0.05).

Figure 8. Co-occurrence network of microbial taxa detected in the four habitats via a high-throughput DNA sequencing (Illumina MiSeq). Nodes represent fungal OTUs, whereas edges represent significant positive correlations between pairs of OTUs. The node size corresponds to the number of connections, and taxa with many correlations are within densely connected areas of the network. Green edges between nodes represent co-presence, while red edges represent mutual exclusion.

Figure 1

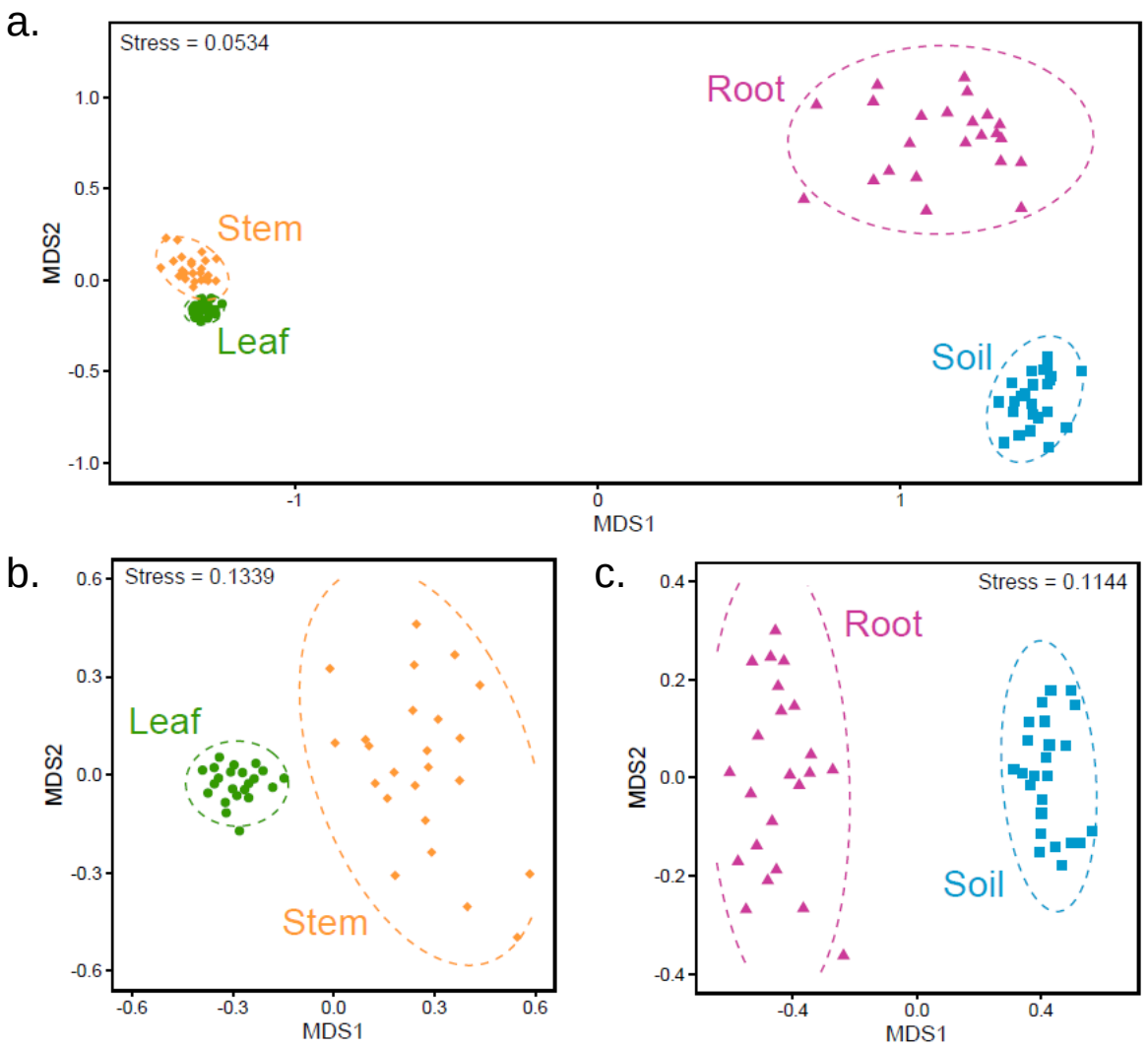
a.
Stress = 0.0534
Root
Stem
Leaf
Soil
MDS1
MDS2
b.
Stress = 0.1339
Leaf
Stem
MDS1
MDS2
c.
Stress = 0.1144
Root
Soil
MDS1
MDS2

Figure 2

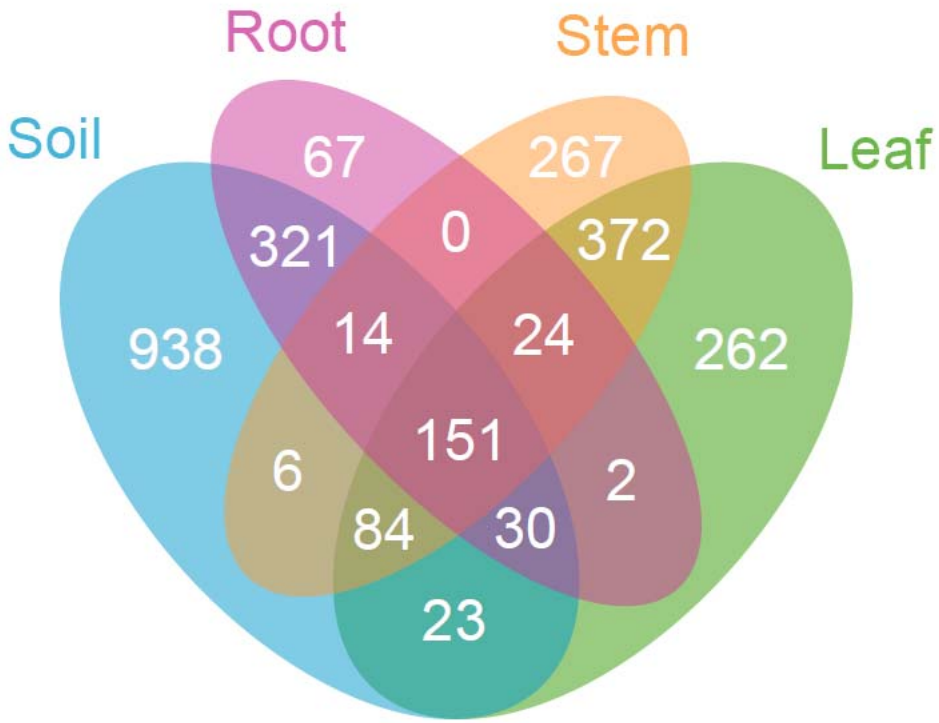

Figure 3

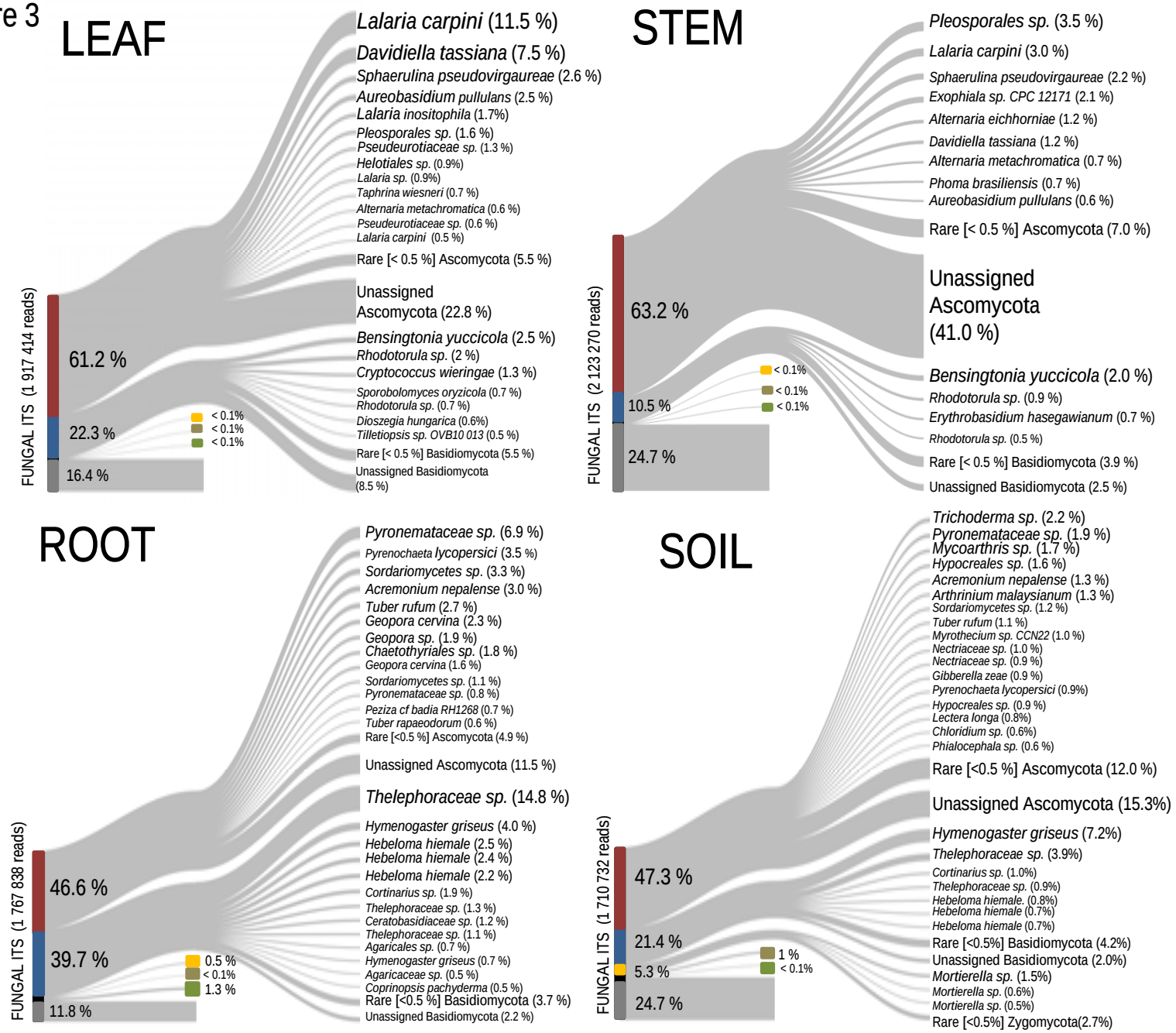
LEAF
FUNGAL ITS (1 917 414 reads)
61.2 %
22.3 %
16.4 %
< 0.1%
< 0.1%
< 0.1%
Lalaria carpini (11.5 %)
Davidiella tassiana (7.5 %)
Sphaerulina pseudovirgaureae (2.6 %)
Aureobasidium pullulans (2.5 %)
Lalaria inositophila (1.7%)
Pleosporales sp. (1.6 %)
Pseudeurotiaceae sp. (1.3 %)
Helotiales sp. (0.9%)
Lalaria sp. (0.9%)
Taphrina wiesneri (0.7 %)
Alternaria metachromatica (0.6 %)
Pseudeurotiaceae sp. (0.6 %)
Lalaria carpini (0.5 %)
Rare [< 0.5 %] Ascomycota (5.5 %)
Unassigned Ascomycota (22.8 %)
Bensingtonia yuccicola (2.5 %)
Rhodotorula sp. (2 %)
Cryptococcus wieringae (1.3 %)
Sporobolomyces oryzicola (0.7 %)
Rhodotorula sp. (0.7 %)
Dioszegia hungarica (0.6%)
Tilletiopsis sp. OVB10 013 (0.5 %)
Rare [< 0.5 %] Basidiomycota (5.5 %)
Unassigned Basidiomycota (8.5 %)
STEM
FUNGAL ITS (2 123 270 reads)
63.2 %
10.5 %
24.7 %
< 0.1%
< 0.1%
< 0.1%
Pleosporales sp. (3.5 %)
Lalaria carpini (3.0 %)
Sphaerulina pseudovirgaureae (2.2 %)
Exophiala sp. CPC 12171 (2.1 %)
Alternaria eichhorniae (1.2 %)
Davidiella tassiana (1.2 %)
Alternaria metachromatica (0.7 %)
Phoma brasiliensis (0.7 %)
Aureobasidium pullulans (0.6 %)
Rare [< 0.5 %] Ascomycota (7.0 %)
Unassigned Ascomycota (41.0 %)
Bensingtonia yuccicola (2.0 %)
Rhodotorula sp. (0.9 %)
Erythrobasidium hasegawianum (0.7 %)
Rhodotorula sp. (0.5 %)
Rare [< 0.5 %] Basidiomycota (3.9 %)
Unassigned Basidiomycota (2.5 %)
ROOT
FUNGAL ITS (1 767 838 reads)
46.6 %
39.7 %
11.8 %
0.5 %
< 0.1%
1.3 %
Pyronemataceae sp. (6.9 %)
Pyrenochaeta lycopersici (3.5 %)
Sordariomycetes sp. (3.3 %)
Acremonium nepalense (3.0 %)
Tuber rufum (2.7 %)
Geopora cervina (2.3 %)
Geopora sp. (1.9 %)
Chaetothyriales sp. (1.8 %)
Geopora cervina (1.6 %)
Sordariomycetes sp. (1.1 %)
Pyronemataceae sp. (0.8 %)
Peziza cf badia RH1268 (0.7 %)
Tuber rapaeodorum (0.6 %)
Rare [<0.5 %] Ascomycota (4.9 %)
Unassigned Ascomycota (11.5 %)
Thelephoraceae sp. (14.8 %)
Hymenogaster griseus (4.0 %)
Hebeloma hiemale (2.5 %)
Hebeloma hiemale (2.4 %)
Hebeloma hiemale (2.2 %)
Cortinarius sp. (1.9 %)
Thelephoraceae sp. (1.3 %)
Ceratobasidiaceae sp. (1.2 %)
Thelephoraceae sp. (1.1 %)
Agaricales sp. (0.7 %)
Hymenogaster griseus (0.7 %)
Agaricaceae sp. (0.5 %)
Coprinopsis pachyderma (0.5 %)
Rare [<0.5 %] Basidiomycota (3.7 %)
Unassigned Basidiomycota (2.2 %)
SOIL
FUNGAL ITS (1 710 732 reads)
47.3 %
21.4 %
5.3 %
24.7 %
1 %
< 0.1%
Trichoderma sp. (2.2 %)
Pyronemataceae sp. (1.9 %)
Mycoarthris sp. (1.7 %)
Hypocreales sp. (1.6 %)
Acremonium nepalense (1.3 %)
Arthrinium malaysianum (1.3 %)
Sordariomycetes sp. (1.2 %)
Tuber rufum (1.1 %)
Myrothecium sp. CCN22 (1.0 %)
Nectriaceae sp. (1.0 %)
Nectriaceae sp. (0.9 %)
Gibberella zeae (0.9 %)
Pyrenochaeta lycopersici (0.9%)
Hypocreales sp. (0.9 %)
Lectera longa (0.8%)
Chloridium sp. (0.6%)
Phialocephala sp. (0.6 %)
Rare [<0.5 %] Ascomycota (12.0 %)
Unassigned Ascomycota (15.3%)
Hymenogaster griseus (7.2%)
Thelephoraceae sp. (3.9%)
Cortinarius sp. (1.0%)
Thelephoraceae sp. (0.9%)
Hebeloma hiemale. (0.8%)
Hebeloma hiemale (0.7%)
Hebeloma hiemale (0.7%)
Rare [<0.5%] Basidiomycota (4.2%)
Unassigned Basidiomycota (2.0%)
Mortierella sp. (1.5%)
Mortierella sp. (0.6%)
Mortierella sp. (0.5%)
Rare [<0.5%] Zygomycota(2.7%)

Figure 4

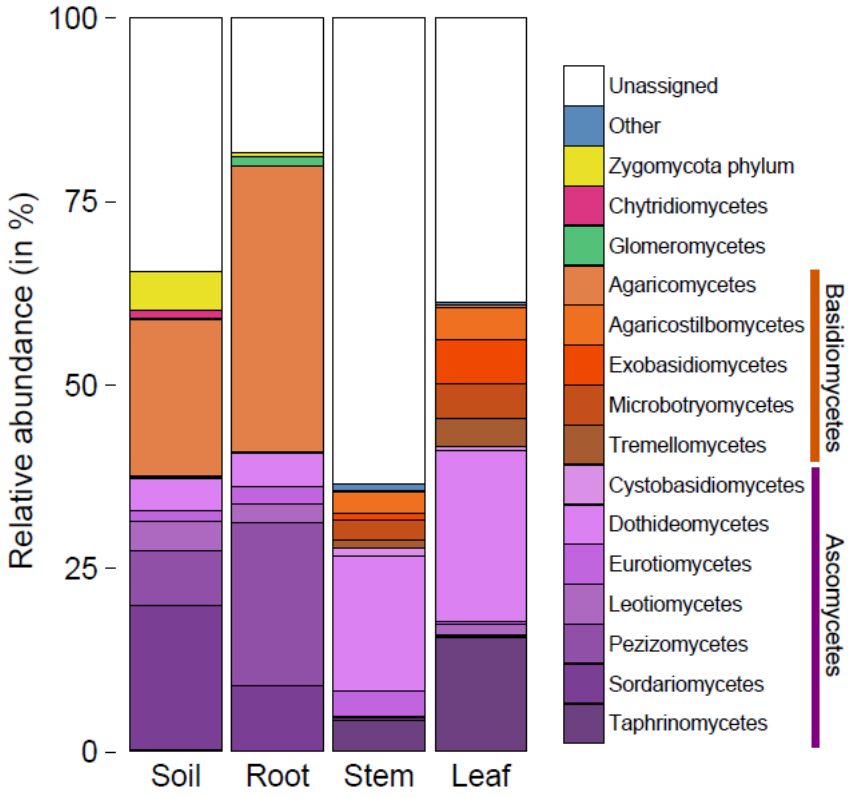
100
75
50
25
0
Relative abundance (in %)
Soil
Root
Stem
Leaf
Unassigned
Other
Zygomycota phylum
Chytridiomycetes
Glomeromycetes
Agaricomycetes
Agaricostilbomycetes
Exobasidiomycetes
Microbotryomycetes
Tremellomycetes
Cystobasidiomycetes
Dothideomycetes
Eurotiomycetes
Leotiomycetes
Pezizomycetes
Sordariomycetes
Taphrinomycetes
Basidiomycetes
Ascomycetes

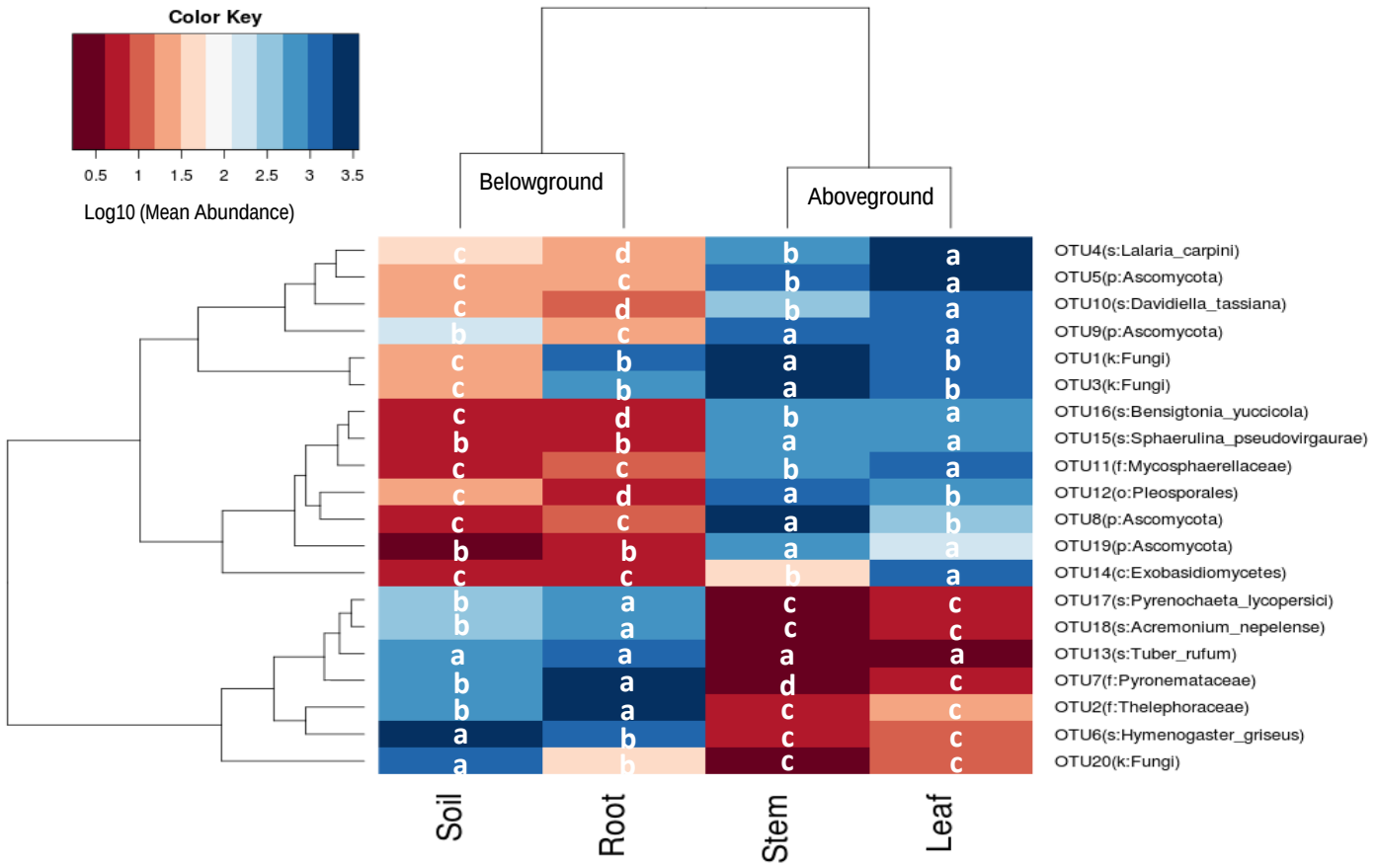
Color Key
0.5
1
1.5
2
2.5
3
3.5
Log10 (Mean Abundance)
Belowground
Aboveground
OTU4(s:Lalaria_carpini)
OTU5(p:Ascomycota)
OTU10(s:Davidiella_tassiana)
OTU9(p:Ascomycota)
OTU1(k:Fungi)
OTU3(k:Fungi)
OTU16(s:Bensigtonia_yuccicola)
OTU15(s:Sphaerulina_pseudovirgaurae)
OTU11(f:Mycosphaerellaceae)
OTU12(o:Pleosporales)
OTU8(p:Ascomycota)
OTU19(p:Ascomycota)
OTU14(c:Exobasidiomycetes)
OTU17(s:Pyrenochaeta_lycopersici)
OTU18(s:Acremonium_nepelense)
OTU13(s:Tuber_rufum)
OTU7(f:Pyronemataceae)
OTU2(f:Thelephoraceae)
OTU6(s:Hymenogaster_griseus)
OTU20(k:Fungi)
Soil
Root
Stem
Leaf

Figure 6

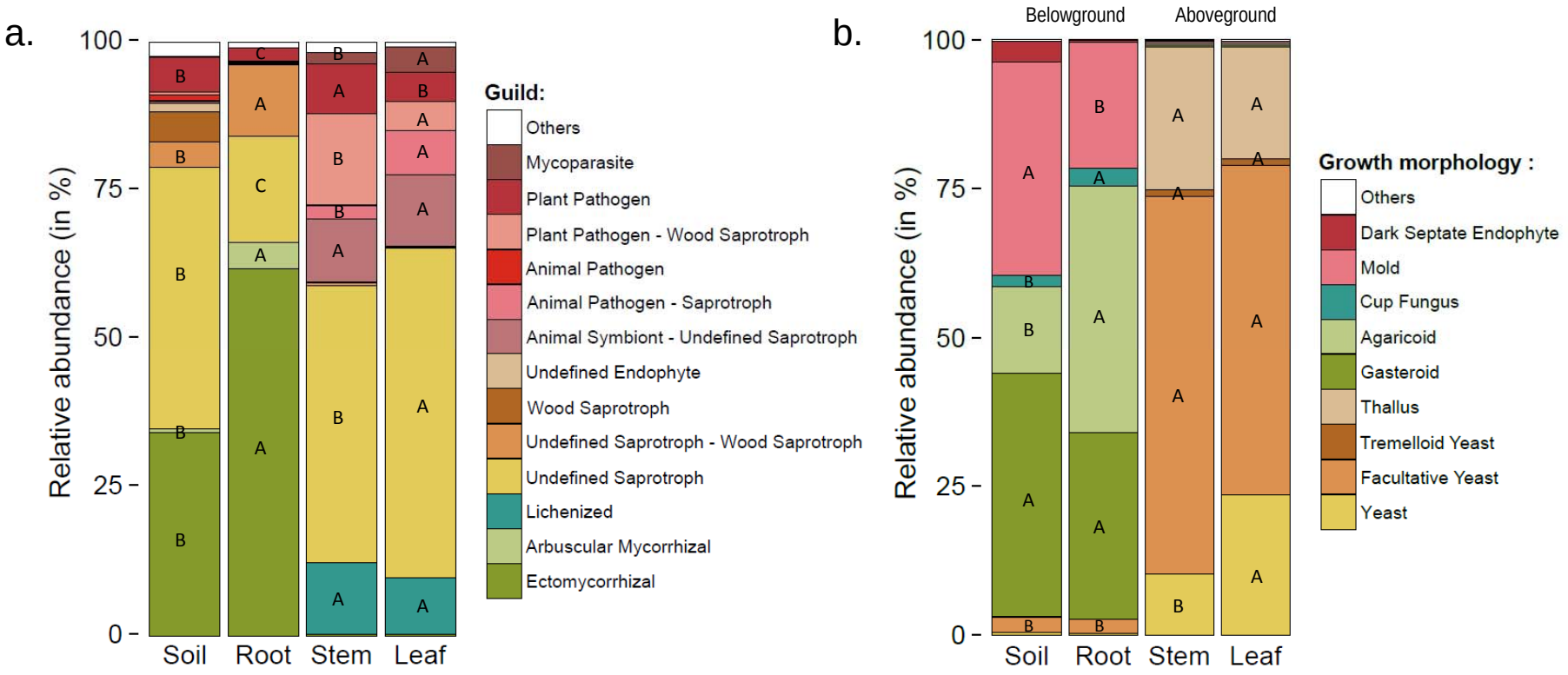
a.
Relative abundance (in %)
100
75
50
25
0
Soil
Root
Stem
Leaf
Guild:
Others
Mycoparasite
Plant Pathogen
Plant Pathogen - Wood Saprotroph
Animal Pathogen
Animal Pathogen - Saprotroph
Animal Symbiont - Undefined Saprotroph
Undefined Endophyte
Wood Saprotroph
Undefined Saprotroph - Wood Saprotroph
Undefined Saprotroph
Lichenized
Arbuscular Mycorrhizal
Ectomycorrhizal
b.
Belowground
Aboveground
Growth morphology :
Others
Dark Septate Endophyte
Mold
Cup Fungus
Agaricoid
Gasteroid
Thallus
Tremelloid Yeast
Facultative Yeast
Yeast

Figure 7

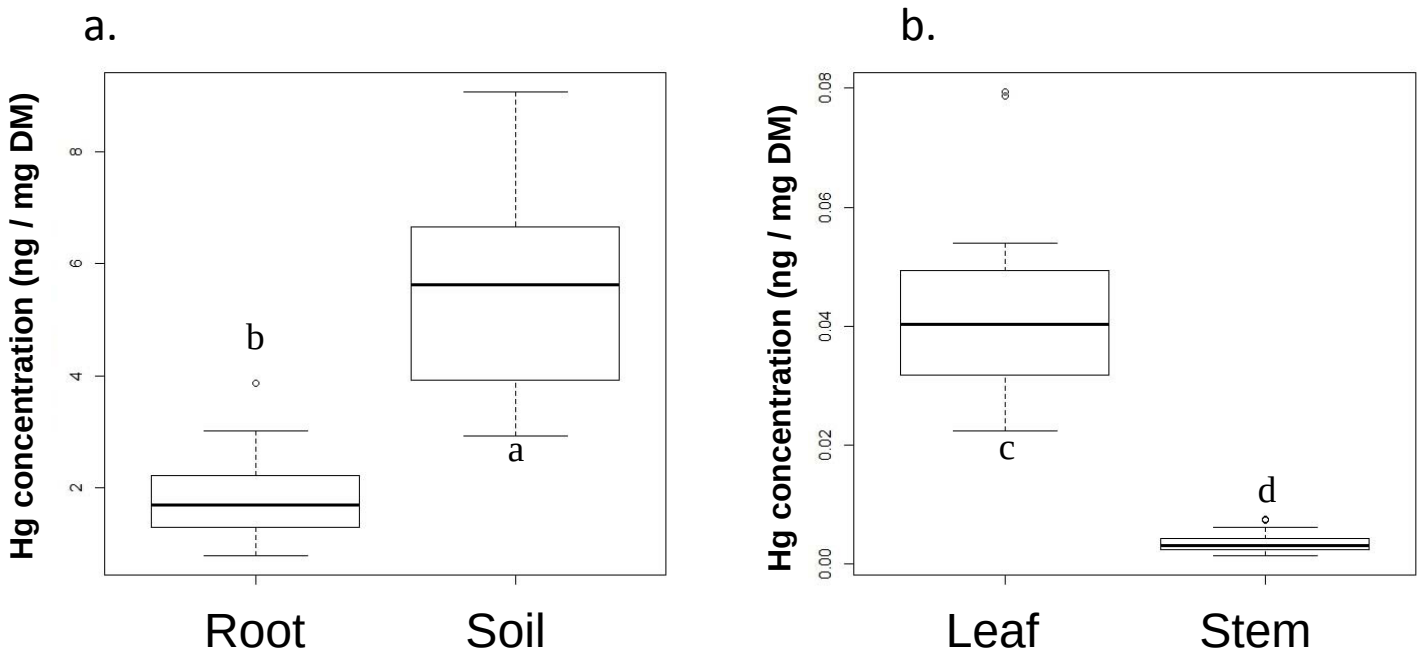
a.
Hg concentration (ng / mg DM)
2
4
6
8
b
a
Root
Soil
b.
Hg concentration (ng / mg DM)
0.00
0.02
0.04
0.06
0.08
c
d
Leaf
Stem

Figure 8

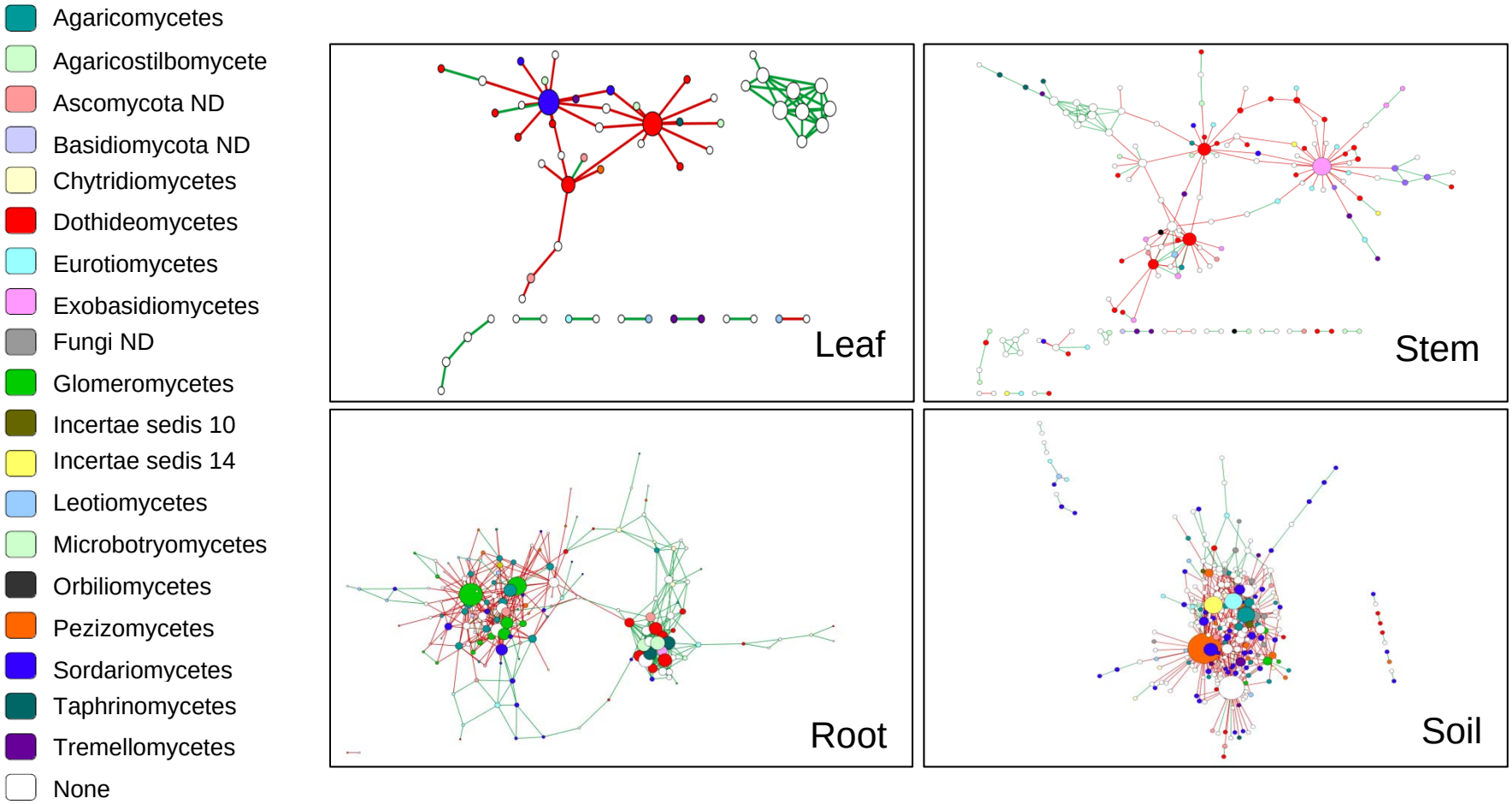
Agaricomycetes
Agaricostilbomycete
Ascomycota ND
Basidiomycota ND
Chytridiomycetes
Dothideomycetes
Eurotiomycetes
Exobasidiomycetes
Fungi ND
Glomeromycetes
Incertae sedis 10
Incertae sedis 14
Leotiomycetes
Microbotryomycetes
Orbiliomycetes
Pezizomycetes
Sordariomycetes
Taphrinomycetes
Tremellomycetes
None
Leaf
Stem
Root
Soil

Table 1. Richness and diversity indices of the fungal communities from the four poplar habitats. All diversity statistics were calculated using an OTU threshold of ≥ 97% sequence similarity on randomly subsampled data at the lower sample size (26,671 reads). Richness was calculated using the number of OTUs and Chao1 estimators. Diversity was estimated from the Shannon-Wiener (H), Inverse Simpson's (1/D) and Shannon Index Evenness (E) indices. Mean values and standard deviations (mean ± SD) are provided for the leaf (n = 22), root (n = 23), and soil and stem (n = 24) samples. Values designated with the same letters were not significantly different (Kruskal-Wallis test, $P < 0.05$).

Habitat	Soil	Root	Stem	Leaf
Mean number of sequences per sample	86,849	88,863	76,863	71,281
Subsample size	26,671	26,671	26,671	26,671
Observed OTUs	785^{a} (± 11)	373^{d} (± 11)	534^{c} (±13)	692^{b} (±17)
Chao estimation	1014^{a} (± 12)	588^{d} (± 16)	709^{c} (± 19)	949^{b} (± 25)
Shannon Index (H)	4.41^{a} (± 0.05)	3.12^{d} (± 0.09)	3.79^{c} (± 0.06)	4.09^{b} (± 0.04)
Inverse Simpson index (1/D)	29.7^{a} (± 2.5)	11.6^{c} (± 1.3)	19.3^{b} (± 1.2)	25.0^{a} (± 1.2)
Shannon Index Evenness (E)	0.661^{a} (± 0.008)	0.527^{d} (± 0.015)	0.604^{c} (± 0.007)	0.626^{b} (± 0.004)

Table 2. Mercury tolerance of fungi isolated from the leaves of poplar tree, expressed by their minimum inhibitory concentration (MIC).

Strain code	Identification	Hg MIC 48h (µM)	Growth form morphology	Isolation medium
Ascomycota Pezizomycotina				
Y93	*Aureobasidium pullulans* (JX462673)	16	Dimorphic	Malt
Y97	*Aureobasidium pullulans* (JX462673)	16	Dimorphic	Malt
Y98	*Aureobasidium pullulans* (JX462673)	16	Dimorphic	Malt
Y100	*Aureobasidium pullulans* (JX462673)	16	Dimorphic	Malt
Ascomycota Saccharomycotina				
M14	*Nakazawaea populi* (KM065946)	32	Yeast	PDA
M15	*Nakazawaea populi* (KM065946)	32	Yeast	PDA
M16	*Nakazawaea populi* (KM065946)	16	Yeast	PDA
M18	*Nakazawaea populi* (KM065946)	32	Yeast	PDA
M19	*Nakazawaea populi* (KM065946)	32	Yeast	PDA
M20	*Nakazawaea populi* (KM065946)	32	Yeast	Malt
M22	*Nakazawaea populi* (KM065946)	32	Yeast	Malt
M23	*Nakazawaea populi* (KM065946)	32	Yeast	Malt
M24	*Nakazawaea populi* (KM065946)	32	Yeast	Malt
M25	*Nakazawaea populi* (KM065946)	32	Yeast	Malt
M26	*Nakazawaea populi* (KM065946)	32	Yeast	Malt

Table 3. Network indices obtained through network analysis based on ITS1 rDNA PCR amplicons from fungal communities of the four habitats (soil, root stem and leaf). All correlations were calculated using CoNet at an OTU threshold of a ≥ 90% sequence similarity on randomly subsampled data at the lower sample size (24,809 reads).

Habitats	Soil	Root	Stem	Leaf
Nodes	237	165	153	57
Edges	444	479	184	69
Network diameter	7.57	8.52	8.58	4.53
Network Conectivity	3.75	5.84	2.41	2.42
Mutual exclusion (%)	80.18	46.13	53.80	44.92
Clustering coefficient	0.13	0.28	0.16	0.13
Network density	0.008	0.012	0.013	0.086
Neighborhood connectivity distribution	23.08	10.20	9.15	6.52
Shortest path length distribution	3.09	4.21	3.75	2.14

Microbial Ecology

Supporting Data

Article title: **Environmental metabarcoding reveals contrasting belowground and aboveground fungal communities from poplar at a Hg phytomanagement site**
Authors: Alexis Durand, François Maillard, Julie Foulon, Hyun S. Gweon, Benoit Valot, Michel Chalot

The following Supporting Information is available for this article:

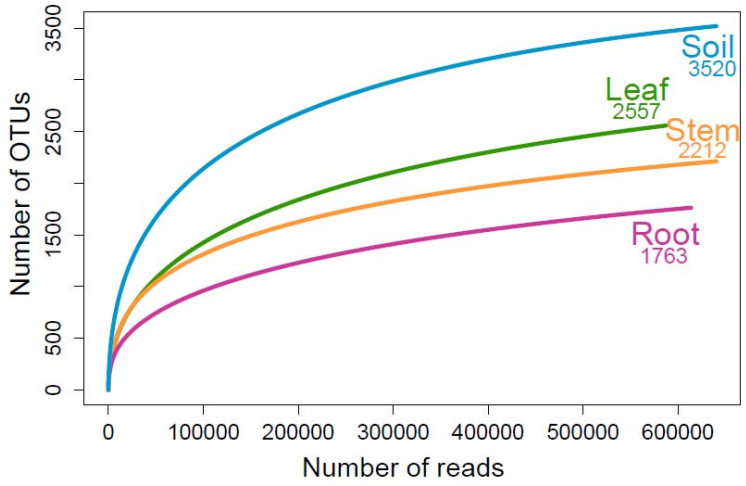

Figure S1. Rarefaction analysis of ITS1 region sequence data for estimating fungal diversity based on a threshold of < 97% sequence similarity for the delineation of operational taxonomic units (OTUs). Comparisons of the fungal communities from the soil, roots, stems and leaves of a *Populus skado* population cultivated under soil Hg contamination (6 ppm).

Table S1. Description of the datasets. Numbers under brackets are the percentage of total effective sequences. “SH”: species hypothesis.

Habitats	Number of samples	Effectives sequences	Phylum assigned sequences	Class assigned sequences	SH assigned sequences	Good's Coverage
Combined dataset	93	7 ,519,254	6,004,207 (79.9%)	4,451,219 (59.2%)	3,915,869 (52.1%)	99.4
Soil	24	1,710,732	1,288,295 (75.3%)	1,099,386 (64.3%)	992,229 (58.0%)	99.4
Root	23	1,767,838	1,558,988 (88.2%)	1,426,069 (80.7%)	1,314,033 (74.33%)	99.5
Stem	24	2,123,270	1,567,354 (73.8%)	752,287 (35.4%)	644,625 (30.36%)	99.4
Leaf	22	1,917,414	1,589,570 (82.9%)	1,173,477 (61.2%)	964,982 (50.33%)	99.1

Table S2. PERMANOVA analyses of the fungal communities associated with poplar considering the factors of habitats, plots and their interactions. For each F test (F), the degrees of freedom (Df), residuals, coefficient of variation (R2) and p-value (P) are indicated.

Scale of analysis	Factor	Df	Residuals	F	R^2	P
Global						
	Habitat	**3**	**88**	**40.655**	**0.581**	**0.001**
	Plot	5	86	1.200	0.065	0.207
	Habitat : Plot	**15**	**76**	**1.450**	**0.093**	**0.018**
Below (soil and root)						
	Habitat	**1**	**44**	**14.304**	**0.245**	**0.001**
	Plot	5	40	1.007	0.112	0.415
	Habitat : Plot	5	40	1.257	0.076	0.112
Above (stem and leaf)						
	Habitat	**1**	**44**	**32.000**	**0.421**	**0.001**
	Plot	5	40	0.800	0.092	0.683
	Habitat : Plot	5	40	1.171	0.072	0.238

Table S3. ANOSIM of the fungal communities associated with the four poplar habitats and their interactions. An ANOSIM R value of 1 indicates complete dissimilarity between groups. Significance levels were estimated (p-value < 0.05).

Habitats	R^2	p-value
Soil: Root: Stem: Leaf	0.86	0.001
Soil: Root: Stem	0.96	0.001
Soil: Root: Leaf	0.96	0.001
Soil: Stem: Leaf	0.84	0.001
Root: Stem: Leaf	0.79	0.001
Soil: Root	0.82	0.001
Soil: Stem	1	0.001
Soil: Leaf	1	0.001
Root: Stem	0.99	0.001
Root: Leaf	0.99	0.001
Stem: Leaf	0.85	0.001

Table S4. Example of FUNguild assignment table

OTU ID	sample	Growth Morphology	taxonomy	Taxon	Taxon Level	Trophic Mode	Guild	Confidence Ranking	Trait	Notes	Citation/Source
ID_exemple1	habitat A	Agaricoid	k__Fungi; p__Basidiomycota; c__Agaricomycetes; o__Agaricales; f__Tricholomataceae; g__Tricholoma; s__Tricholoma_scalpturatum|SH193992,06FU	Tricholoma	13	Symbiotroph	Ectomycorrhizal	Highly Probable	NULL	NULL	Rinaldi AC, et al, 2008, Fungal Diversity 33:1-45; Tedersoo L, et al, 2010, Mycorrhiza 20:217-263; http://mycorrhizas,info/ecmf,html

Table S5. The ten keystone species in each habitat, characterized by their number of connections, shown by the number of total degrees, as either positive (+) or negative (-), and their relative abundance (%).

habitat	class	genus	OTU	degree	+	-	Abundance (%)
Leaf	*Sordariomycetes*	*Myrothecium*	ITS-10-33105	13	1	12	0.013
	Dothideomycetes	*unassigned*	ITS-22-43074	12	0	12	0.017
	unassigned	*unassigned*	ITS-24-223674	8	8	0	0.253
	unassigned	*unassigned*	ITS-17-15719	7	7	0	0.469
	unassigned	*unassigned*	ITS-24-207298	7	7	0	0.636
	Dothideomycetes	*Dothideomycetes ND*	ITS-25-24380	7	1	6	0.015
	unassigned	*unassigned*	ITS-14-9158	6	6	0	0.242
	unassigned	*unassigned*	ITS-18-89496	6	6	0	0.358
	unassigned	*unassigned*	ITS-20-53698	6	6	0	0.191
	unassigned	*unassigned*	ITS-24-147537	6	6	0	0.115
Stem	*Exobasidiomycetes*	*Exobasidiomycetes ND*	ITS-6-10425	28	0	28	0.159
	Dothideomycetes	*Pleosporales ND*	ITS-39-17431	18	4	14	0.011
	Dothideomycetes	*unassigned*	ITS-96-2475	17	1	16	0.015
	Dothideomycetes	*Sclerostagonospora*	ITS-18-79499	12	4	8	0.016
	unassigned	*unassigned*	ITS-28-13546	11	3	8	0.048
	unassigned	*unassigned*	ITS-18-89496	9	9	0	0.052
	unassigned	*unassigned*	ITS-14-9158	8	8	0	0.038
	unassigned	*unassigned*	ITS-24-207298	8	8	0	0.091
	unassigned	*unassigned*	ITS-33-23754	8	2	6	0.013
	unassigned	*unassigned*	ITS-17-15719	7	7	0	0.065
Root	*Glomeromycetes*	*Glomeraceae ND*	ITS-56-66798	31	4	27	0.018
	Glomeromycetes	*Entrophospora*	ITS-84-41503	25	2	23	0.040
	unassigned	*unassigned*	ITS-26-60015	19	19	0	0.080
	Microbotryomycetes	*Rhodotorula*	ITS-45-24611	19	19	0	0.010
	Dothideomycetes	*unassigned*	ITS-20-30632	18	18	0	0.039
	Taphrinomycetes	*Lalaria*	ITS-24-161008	18	18	0	0.015
	unassigned	*unassigned*	ITS-70-85660	18	5	13	0.020
	Taphrinomycetes	*Lalaria*	ITS-19-64636	17	17	0	0.078
	Dothideomycetes	*unassigned*	ITS-32-60520	17	17	0	0.030
	Agaricomycetes	*Sebacinaceae ND*	ITS-67-12914	17	1	16	0.086
Soil	*Pezizomycetes*	*Peziza*	ITS-75-68665	63	2	61	0.313
	none	*none*	ITS-93-78141	48	3	45	0.106
	Incertae sedis 14	*Hymenula*	ITS-77-41916	32	5	27	0.025
	Eurotiomycetes	*Exophiala*	ITS-83-24561	30	1	29	0.036
	Agaricomycetes	*Ceratobasidiaceae ND*	ITS-80-41094	29	1	28	0.020
	unassigned	*unassigned*	ITS-57-30026	22	1	21	0.052
	Sordariomycetes	*Lasiosphaeriaceae ND*	ITS-96-29396	22	4	18	0.028
	Fungi unidentified 1	*Fungi ND 1.1*	ITS-80-44171	15	1	14	0.080
	unassigned	*unassigned*	ITS-89-5134	15	2	13	0.015
	Sordariomycetes	*unassigned*	ITS-93-46680	14	8	6	0.013